Electronic supporting information for

Impact of the Schiff Base Ligand Substituents on the Solid State and Solution Properties in Eleven Iron(III) Complexes

Lukáš Pogány,[a] Barbora Brachňaková,[a] Petra Masárová,[a] Ján Moncol,[a] Ján Pavlik,[a] Miroslav Gál,[b] Milan Mazúr,[c] Radovan Herchel,[d] Ivan Nemec,[d] Ivan Šalitroš,[a,d*]

a) Department of Inorganic Chemistry, Faculty of Chemical and Food Technology, Slovak University of Technology in Bratislava, Bratislava SK-81237, Slovakia, *e-mail: ivan.salitros@stuba.sk
b) Department of Inorganic Technology, Faculty of Chemical and Food Technology, Slovak University of Technology, Bratislava-81237, Slovakia
c) Department of Physical Chemistry, Faculty of Chemical and Food Technology, Slovak University of Technology in Bratislava, Bratislava SK-81237, Slovakia
d) Department of Inorganic Chemistry, Faculty of Science, Palacký University, 17. listopadu 12, 771 46 Olomouc, Czech Republic

S1. Experimental part

General

All purchased chemicals and solvents (methanol, acetone, ethanol, acetonitrile and diethyl ether) were used as received without any further purification. IR spectra were measured by the ATR technique or in KBr pellets in the 4000 – 400 cm^{-1} region (Magna FTIR 750. Nicolet). Electronic spectra were recorded in the acetonitrile solutions at the concentration (1 ± 0.1)10^{-4} mol dm^{-3} (except **7** - 2. 10^{-4} mol dm^{-3}) on Specord 250 plus Analytical Jena in the range of 800 – 200 nm. Elemental analysis of carbon, hydrogen and nitrogen was carried out by an automated analyser (Vario Micro Cube). Electrochemical measurements were carried out using a three-electrode electrochemical cell system for cyclic and square wave (SW) voltammetry. The reference electrode (RE). Ag|AgCl|LiCl, was separated from the test solution by a salt bridge. The working electrode (WE) was Pt disc electrode. The counter electrode (CE) was a platinum foil with area ca 400× higher than area of WE. Oxygen was removed from the solution by passing a stream of argon for at least 5 min. before each experiment. All electrochemical experiments were performed at 25±1 °C in 0.1 M anhydrous LiCl (puriss. p. a. Sigma-Aldrich) dissolved in dry absolute ethanol (Centralchem). Absolute ethanol was dried over molecular sieve (Sigma-Aldrich) for at least 5 days prior to experiments.

Synthesis

The general synthesis of the complexes **1**–**10** of formula [Fe(Ln)Cl] (where Ln is a double deprotonated form of the corresponding SB ligand H_2Ln; n=1-10; Scheme S1) consists of two steps. At first, the SB condensation between the corresponding aliphatic triamine (5 mmol; dissolved in 15 cm^3 of CH_3OH; *N*-(2-aminoethyl)ethane-1,2-diamine for compounds **1** – **4**; *N*-(2-aminoethyl)propane-1,3-diamine for complexes **5** and **6**; *N*-(3-aminopropyl)propane-1,3-diamine for compounds **7** and **8** and *N*-(3-aminopropyl)-*N*-methylpropane-1,3-diamine for **9** and **10**) and corresponding substituted aromatic 2-hydroxycarbaldehyde (10 mmol; dissolved in 15 cm^3 of CH_3OH; 2-hydroxy-1-naphthaldehyde for complexes **1** and **9**; 1-(2-hydroxynaphthalen-1-yl)ethanone for compound **2**; 3-methoxysalicylaldehyde for complex **3**; 5-bromosalicylaldehyde for complexes **4**, **7**; 3-ethoxysalicylaldehyde for complex **5**; and 6-bromo-3-methoxysalicylaldehyde for complexes **6**, **8** and **10**) is taking place. Next, the yellow solution of *in situ* prepared SB ligand H_2Ln is stirred for 30 minutes at 50°C and addition of stoichiometric amount of $FeCl_3 \cdot 6H_2O$ (5 mmol, dissolved in 10 cm^3 of CH_3OH) caused intensive colour change to dark violet. Hydrochloric acid as the side product of iron(III) complexation was neutralized with triethylamine (12 mmol; dissolved in 10 cm^3 of CH_3OH) and the reaction mixture was stirred at 80 °C for another 2 hours, cooled down to 0 °C and dark violet or black polycrystalline product was filtered off, washed with a small amount of cold methanol, diethyl ether and dried under vacuum. Single-crystals suitable for X-ray diffraction analysis were obtained by recrystallisation of polycrystalline powders from acetone (for complexes **1**, **6**, **7c**, **8**, **9** and **10**), methanol (complex **2**, **3** and **5**) and from methanol:acetonitrile mixture (1:1 for **4** or 1:2 for **7t**).

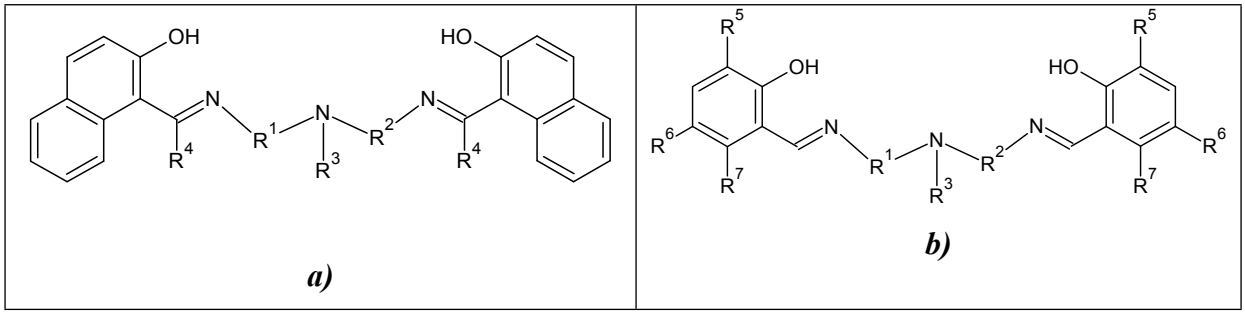

Scheme S1 Molecular structures of *in situ* prepared SB ligands: ***a)*** **H_2L1** = *N,N′*-bis(2-hydroxynaphtyllidene)-1,5-diamino-3-azapentane. R^1=R^2=CH_2-CH_2, R^4=R^3=H; **H_2L2** = (1–(3–(2–(2–hydroxynaphtalene–1–yl)metyleneaminoethylamino)propylimino)-metyl)naphthalene-2-ol. R^1 = R^2= CH_2-CH_2, R^3=H, R^4 =CH_3; **H_2L9** = *N,N′*-bis(2-hydroxynaphtyllidene)-1,7-diamino-4-aza-(4-methyl)heptane; R^1 = R^2= CH_2-CH_2-CH_2, R^3 = CH_3, R^4 = H; **b) H_2L3** = *N,N′*- bis(3-methoxy-2-hydroxybenzylidene)-1,5-diamino-3-azapentane). R^1 = R^2= CH_2-CH_2, R^5=O-CH_3, R^3= R^6= R^7=H; **H_2L4** = *N,N′*-bis(5-bromo-2-hydroxybenzylidene)-1,5-diamino-3-azapentane; R^1 = R^2= CH_2-CH_2, R^6=Br, R^3=R^7=H; **H_2L5** = *N,N′*-bis(3-ethoxy-2-hydroxybenzylidene)-1,6-diamino-3-azahexane; R^1=CH_2-CH_2-CH_2, R^2= CH_2-CH_2, R^5=O-CH_2-CH_3, R^3= R^6= R^7=H; **H_2L6** = *N,N′*-bis(6-bromo-3-methoxy-2-hydroxybenzylidene)-1,6-diamino-3-azahexane); R^1=CH_2-CH_2-CH_2, R^2= CH_2-CH_2, R^5=O-CH_3, R^7=Br, R^3= R^6=H; **H_2L7** = *N,N′*-bis(5-bromo-2-hydroxybenzylidene)-1,7-diamino-4-azaheptane; R^1=R^2= CH_2-CH_2-CH_2, R^6=Br, R^3= R^7=H; **H_2L8** = *N,N′*-bis(6-bromo-3-methoxy-2-hydroxybenzylidene)-1,7-diamino-4-azaheptane); R^1= R^2=CH_2-CH_2-CH_2, R^5=O-CH_3, R^7=Br, R^3=R^6=H; **H_2L10** = *N,N′*-bis(6-bromo-3-methoxy-2-hydroxybenzylidene)-1,7-diamino-4-aza-(4-methyl)heptane); R^1= R^2=CH_2-CH_2-CH_2, R^3=CH_3, R^5=O-CH_3, R^7=Br, R^6=H.

Complex **1**: FTIR (ATR; ν /cm^{-1}): 3271 (w, N-H); 3139, 3052, 3028 (w, C_{ar}-H); 2918, 2981, 2866 (w, C_{al}-H); 1715 (m, C=O); 1614, 1601, 1540, 1508 (s, C=N and C=C). UV-VIS (acetonitrile, λ_{max}/nm): 237; 302; 329; 536. Elemental analysis for [Fe(L1)Cl]·CH_3COCH_3 ($C_{29}H_{29}ClFeN_3O_3$; M_w= 558.86 g mol^{-1}) found % (expected %): C 61.95 (62.33); N 7.55 (7.52); H 5.28 (5.23). Yield: 85 %.

Complex **2:** FTIR (ATR; ν /cm^{-1}): 3204 (m, N-H); 3062, 3053, 3023 (w, C_{ar}-H); 2966, 2964, 2917, 2873 (w, C_{al}-H); 1614, 1597, 1536, 1501 (s, C=N and C=C). UV-VIS (acetonitrile, λ_{max}/nm): 238; 293; 328; 535. Elemental analysis for [Fe(L2)Cl] ($C_{28}H_{27}ClFeN_3O_2$; M_w= 528.83 g mol^{-1}) found % (expected %): C 64.00 (63.59); N 7.50 (7.95); H 5.00 (5.15). Yield 90 %.

Complex **3:** FTIR (ATR; ν /cm^{-1}): 3154 (w, N-H); 2989 (w, C_{ar}-H); 2929, 2900, 2872, 2832 (w, C_{al}-H); 1633, 1620, 1598, 1549 (s, C=N and C=C). UV-VIS (acetonitrile, λ_{max}/nm): 232; 271; 333; 537. Elemental analysis for [Fe(L3)Cl] ($C_{20}H_{23}ClFeN_3O_4$; M_w= 460.71 g mol^{-1}) found % (expected %): C 51.92 (52.14); N 9.05 (9.12); H 4.89 (5.03). Yield: 80 %.

Complex **4**: FTIR (ATR; ν /cm^{-1}): 3473 (w, O-H); 3131 (w, N-H); 3041, 3012 (w, C_{ar}-H); 2929, 2867 (w, C_{al}-H); 1619, 1588, 1529 (s, C=N and C=C). UV-VIS (acetonitrile, λ_{max}/nm): 225; 236; 304; 316; 507. Elemental analysis for [Fe(L4)Cl]·CH_3OH ($C_{19}H_{21}Br_2ClFeN_3O_3$, M_w= 590.51 g mol^{-1}) found % (expected %): C 38.89 (38.65); N 6.95 (7.12); H 3.50 (3.58). Yield: 82 %.

Complex **5:** FTIR (ATR; ν /cm^{-1}): 3201 (w, N-H); 3060, 3039, 3024 (w, C_{ar}-H); 2968, 2952, 2931, 2900, 2860 (w, C_{al}-H); 1632, 1615, 1595, 1547 (s, C=N and C=C). UV-VIS (acetonitrile, λ_{max}/nm): 232; 270; 336; 545. Elemental analysis for [Fe(L5)Cl] ($C_{23}H_{29}ClFeN_3O_4$; M_w= 502.79 g mol^{-1}) found % (expected %): C 54.37 (54.94); N 8.22 (8.36); H 5.92 (5.81). Yield 80 %.

Complex **6**: FTIR (ATR; ν /cm^{-1}): 3217 (w, N-H); 3098, 3052 (w, C_{ar}-H); 2964, 2928, 2907, 2874, 2860, 2839 (w, C_{al}-H);1635, 1605, 1583, 1539 (s, C=N and C=C). UV-VIS (acetonitrile, λ_{max}/nm): 238; 279; 343; 545. Elemental analysis for [Fe(L6)Cl] ($C_{21}H_{23}ClFeBr_2N_3O_4$; M_w= 632.53 g mol^{-1}) found % (expected %): C 40.02 (39.88); N 6.79 (6.64); H 3.70 (3.67). Yield: 92 %.

Complex **7t** FTIR (ATR/cm^{-1}): 3241 (w, N-H); 3041 (w, C_{ar}-H); 2961, 2923, 2861, 2800 (w, C_{al}-H); 1616, 1587, 1523 (s, C=N and C=C). UV-VIS (acetonitrile, λ_{max}/nm): 223; 236; 314; 325; 459; 514. UV-VIS (nujol, λ_{max}/nm): 237; 324; 448; 524. Elemental analysis for [Fe(L7)Cl] ($C_{20}H_{21}Br_2ClFe_2N_3O_2$; M_w= 642.35 g mol^{-1}) found % (expected %): C 37.62 (37.40), N 6.74 (6.54%),

3.42 H (3.30%).

Complex **7c** FTIR (ATR/cm^{-1}): FTIR (ATR/cm^{-1}): 3231(w, N-H); 3045 (w, C_{ar}-H); 2945, 2923, 2866, 2837 (w, C_{al}-H); 1624, 1615, 1588, 1523 (s, C=N and C=C). UV-VIS (nujol, λ_{max}/nm): 245; 336; 473; 520. Elemental analysis for [Fe(L7)Cl] ($C_{20}H_{21}Br_2ClFe_2N_3O_2$; M_w= 642.35 g mol^{-1}) found % (expected %): C 37.52 (37.40), N 6.66 (6.54), 3.50 H(3.30). Yield: 89 %.

Complex **8**: FTIR (ATR; /cm^{-1}): 3487 (w, O-H); 3130 (w, N-H); 3055, 3000 (w, C_{ar}-H); 2927, 2907, 2865, 2853, 2832 (w, C_{al}-H); 1611, 1585, 1542 (s, C=N and C=C). UV-VIS (acetonitrile, λ_{max}/nm): 236; 272; 361; 548. Elemental analysis for [Fe(L8)Cl]·H_2O ($C_{22}H_{27}ClFeBr_2N_3O_5$; M_w= 664.57 g mol^{-1}) found % (expected %): C 39.98 (39.76); N 6.45 (6.32); H 4.23 (4.10). Yield: 88 %.

Complex **9**: FTIR (KBr; /cm^{-1}): 3048 (w, C_{ar}-H); 2921, 2825 (w, C_{al}-H); 1601, 1538, 1506, 1506 (s, C=N and C=C). UV-VIS (acetonitrile, λ_{max}/nm): 238; 304; 340; 387; 560. Elemental analysis for [Fe(L9)Cl] ($C_{29}H_{29}ClFeN_3O_2$; M_w= 542.86 g mol^{-1}) found % (expected %): C 63.56 (64.16); N 7.53 (7.74); H 5.40 (5.38). Yield: 92 %.

Complex **10**: FTIR (ATR; /cm^{-1}): 3419 (w, O-H); 2996 (w, C_{ar}-H); 2972, 2944, 2909, 2881, 2855, 2829 (w, C_{al}-H); 1715 (m, C=O); 1609, 1586, 1540 (s, C=N and C=C). UV-VIS (acetonitrile, λ_{max}/nm): 239; 268; 362; 559. Elemental analysis for [Fe(L10)Cl]·H_2O·0.5CH_3COCH_3 ($C_{25}H_{32}ClFeBr_2N_3O_6$; M_w= 707.64 g mol^{-1}) found % (expected %): C 41.75 (41.55); N 5.60 (5.95); 4.60 H (4.55). Yield: 74 %.

Crystal structure determination

The data collection for **2**, **4–9** was performed by Oxford Diffraction Xcalibur S diffractometer with Sapphire 2 CCD detector and graphite-monochromatized MoKα radiation (λ = 0.71073 Å). Intensity data for **3** and **10** were collected by Oxford Diffraction Gemini R diffractometer with Rubby CCD detector and graphite-monochromatized MoKα radiation (λ = 0.71073 Å). The data collection for **1** at 100K and **5** at 293 K were done by Stoe StadiVari diffractometer using Pilatus 300K HPAD detector and microfocus source Xenocs Genix3D Cu HF with CuKα radiation (λ = 1.54186 Å).

The structures were solved by direct methods using the programs SHELXS-97,[1] SHELXT [2] or SIR-2011[3] and refined by the full-matrix least squares method on all F^2 data using program SHELXL (ver. 2018/3).[3] Geometrical analyses were performed using SHELXL. The single crystal suite OLEX2 was used an integrated system for all crystallographic programs and software for preparing the material for publication.[1,4,5]

The crystal structure **5** shows phase transition. Discrete positional disorders of SB ligands were observed in crystal structure of **5(*P*2$_1$/c)** (site occupancy 0.349(4)/0.651(4)), **5(*P*-1)** (site occupancy 0.481(6)/0.519(6) and 0.4778(19)/0.5222(19) for two crystallographic independent complex molecules). The disordered groups are modelled using SADI, EADP and RIGU commands of SHELXL. The disordered parts of **5(P2$_1$/c)** have been modelled using restrained distances of Fe1–N/O with sigma of 0.002, and restrained distances of C–O, C–N and C–C with sigma of 0.004. The disordered parts of **5(*P*-1)** have been modelled using restrained distances of Fe1–N/O with sigma of 0.002, and restrained distances of C–O, C–N and C–C with sigma of 0.02. Rigid body restrains have been used for atoms of disorders. The U_{aniso} of the equivalent atoms of two part of disorder have been also constrained.

Unresolved disordered solvent molecules of **2** and **10** at 293 K have been masked using bulk-solvent correction in OLEX2.[6,7] All non-hydrogen atoms of the complexes were refined anisotropically as independent atoms. Hydrogen atoms were geometrically optimized into idealized positions. The crystal parameters data collection and refinement are summarized in Table 1.

Magnetic measurements

Magnetic investigations were performed by a SQUID magnetometer (MPMS-XL7, Quantum Design) in the RSO mode of detection. In all cases, the temperature dependence of magnetic moment was recorded at external field 0.1 T and the temperature sweeping rate was 1 K/min. The gelatine-made capsules as sample holders were used and their small diamagnetic contribution is negligible in the overall magnetization, which was dominated by the sample. The diamagnetic corrections to the molar magnetic susceptibilities were applied using Pascal constants.[8] The fitting of the magnetic susceptibility and magnetization was performed with the help of a home-made program.

EPR spectroscopy

The solid-state X-band (ca 9.4 GHz, hν ≈ 0.3 cm^{-1}) EPR spectra of powder complexes **1 - 10** were measured on EMX EPR spectrometer (Bruker, Germany) operating with 100 kHz modulation technique at temperature of 293 K and 98 K. The thin-walled quartz EPR sample tubes (Bruker) was used. The temperature was controlled by Bruker temperature control unit ER 4111 VT. The first derivative EPR spectra were processed, evaluated and analyzed by the original software as follows: WinEPR,[9] SimFonia,[10] „Spin“[11] and „Visual Rhombo” [12]. The spin Hamiltonian parameter values obtained from the experimental EPR spectra were then further refined by computer simulation.

Computational details

The DFT calculations were carried out with the ORCA 4.0.1.2[13] package. The magnetic properties were investigated with the hybrid X3LYP functional[14] and the scalar relativistic correction was included by applying the second order Douglass–Kroll–Hess approach (DKH).[15] The polarized, relativistically recontracted triple-ζ quality basis set DKH-def2-TZVP proposed by Ahlrichs and co-workers was used for all atoms.[16] The chain-of-spheres approximation to exact exchange (RIJCOSX)[17] was used with an automatically generated auxiliary basis set.[18] Increased integration grid (Grid5 in ORCA convention) and fine convergence criteria (verytightscf and veryslowconv) were employed in all calculations. For all investigated systems the calculations were based on the experimentally determined X-ray structures, except of positions of hydrogen atoms, which were optimized using the PBEh-3c method.[19] The reductional potential was studied with wB97X-D3 range-separated hybrid GGA functional with empirical dispersion correction included.[20] The relativistic effects were included with a zero order regular approximation (ZORA)[20] and the scalar relativistic contracted version of ZORA-def2-TZVP(-f) basis functions for all atoms except carbon and hydrogen for which ZORA-def2-SVP basis set was used.[21] The molecular geometries were optimized both for neutral and reduced species and the analytical calculations of the molecular vibrations were used for thermochemistry. The molecular coordinates of the optimized structures are attached as extra supplementary .xyz files.

S2. Infrared spectra of reported compounds

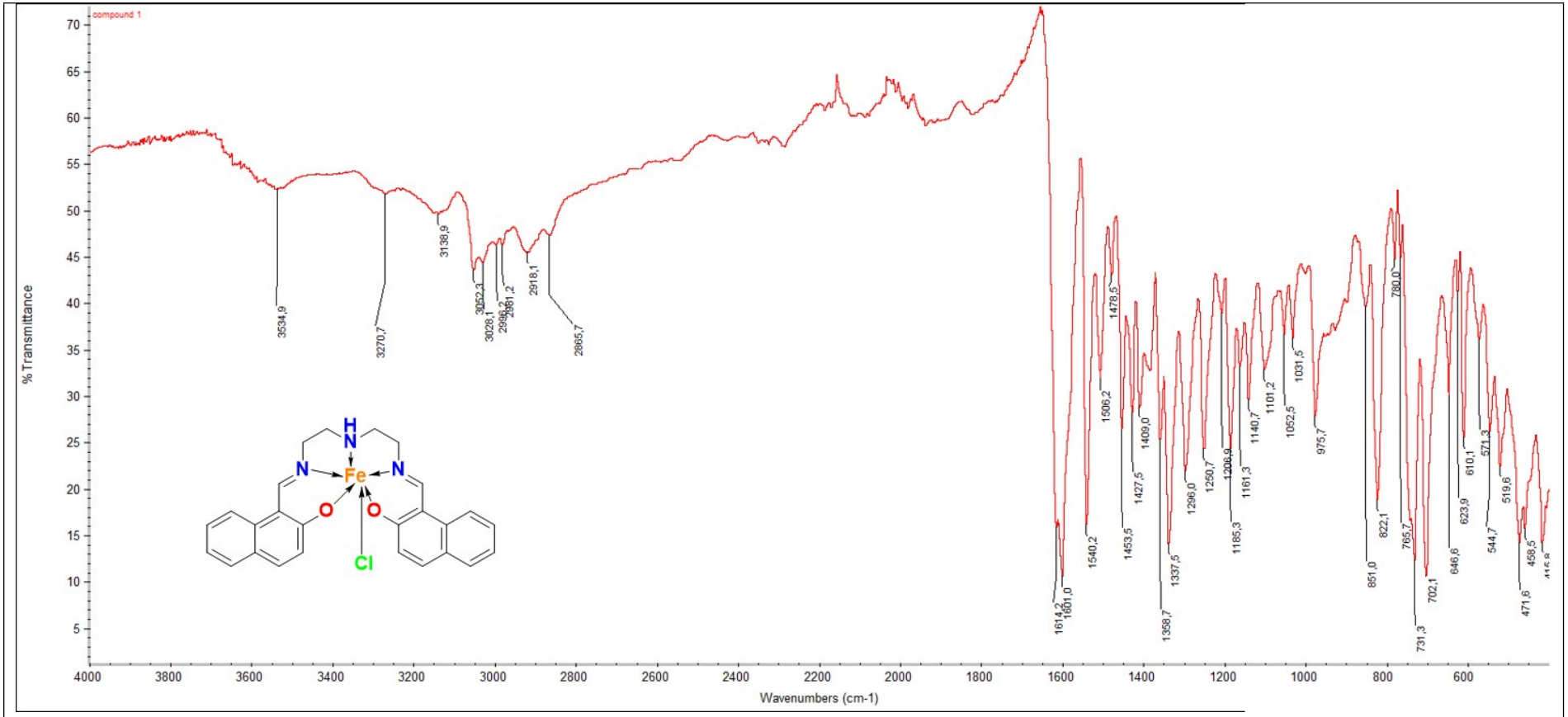

Compound **1**

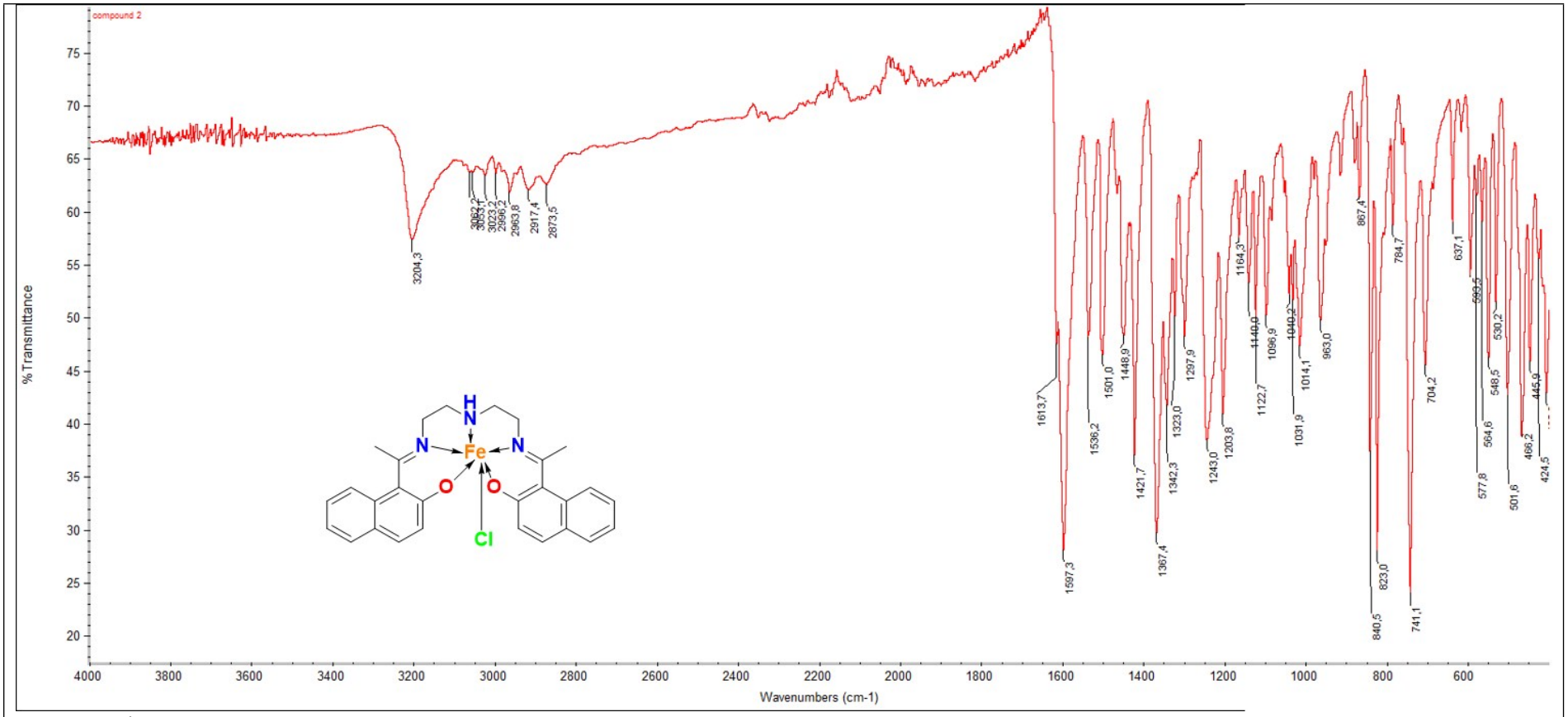
compound 2
% Transmittance
Wavenumbers (cm-1)
3204,3
2963,8
2917,4
2873,5
1613,7
1597,3
1536,2
1501,0
1448,9
1421,7
1367,4
1342,3
1323,0
1297,9
1243,0
1203,8
1164,3
1122,7
1096,9
1031,9
1014,1
963,0
867,4
840,5
823,0
784,7
741,1
704,2
637,1
577,8
564,6
548,5
530,2
501,6
466,2
445,9
424,5
H
N
N
Fe
N
O
O
Cl

Compound **2**

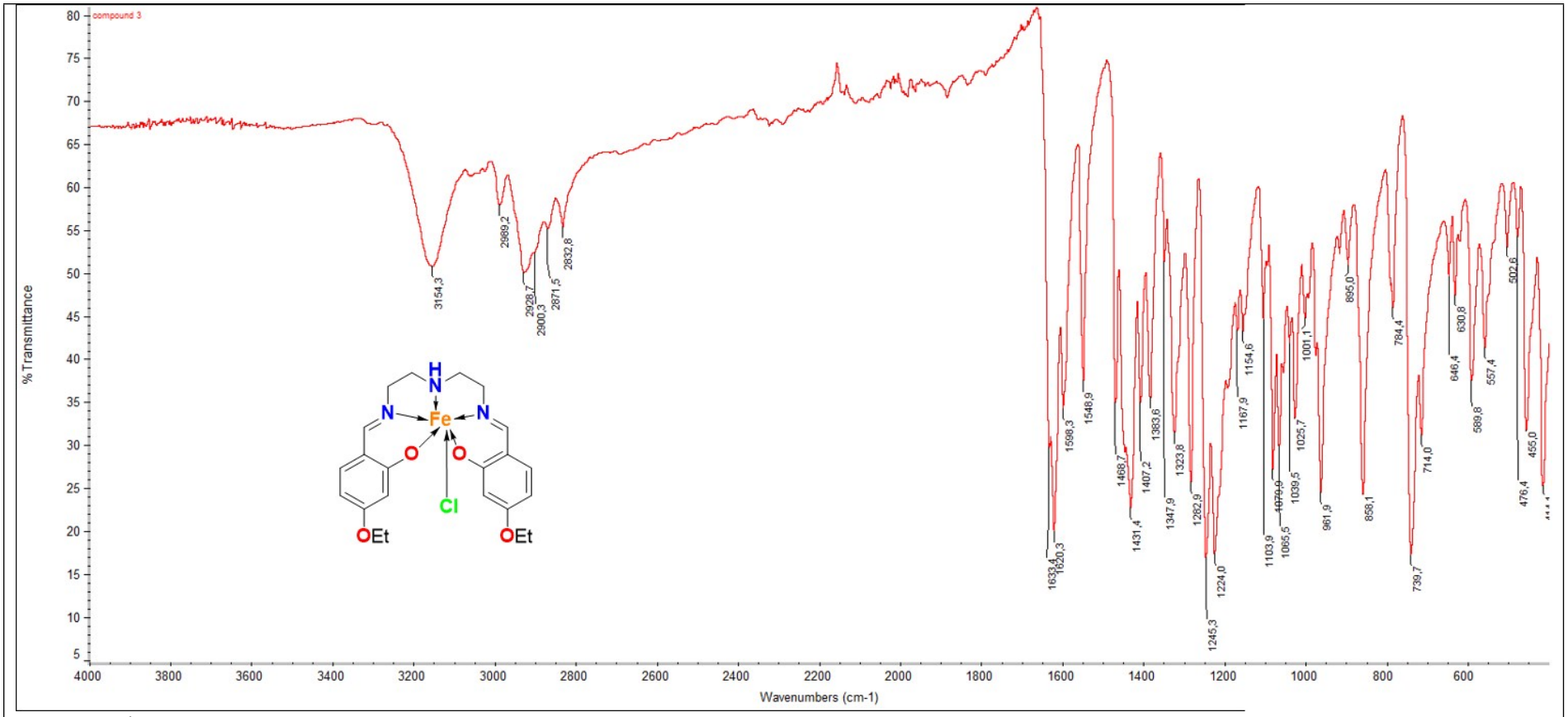
compound 3
% Transmittance
Wavenumbers (cm-1)
3154,3
2989,2
2928,7
2900,3
2871,5
2832,8
1633,4
1620,3
1598,3
1548,9
1468,7
1431,4
1407,2
1383,6
1347,9
1323,8
1282,9
1245,3
1224,0
1167,9
1154,6
1103,9
1079,9
1065,5
1039,5
1025,7
1001,1
961,9
895,0
858,1
784,4
739,7
714,0
646,4
630,8
589,8
557,4
502,6
476,4
455,0
H
N
N
N
Fe
O
O
Cl
OEt
OEt

Compound **3**

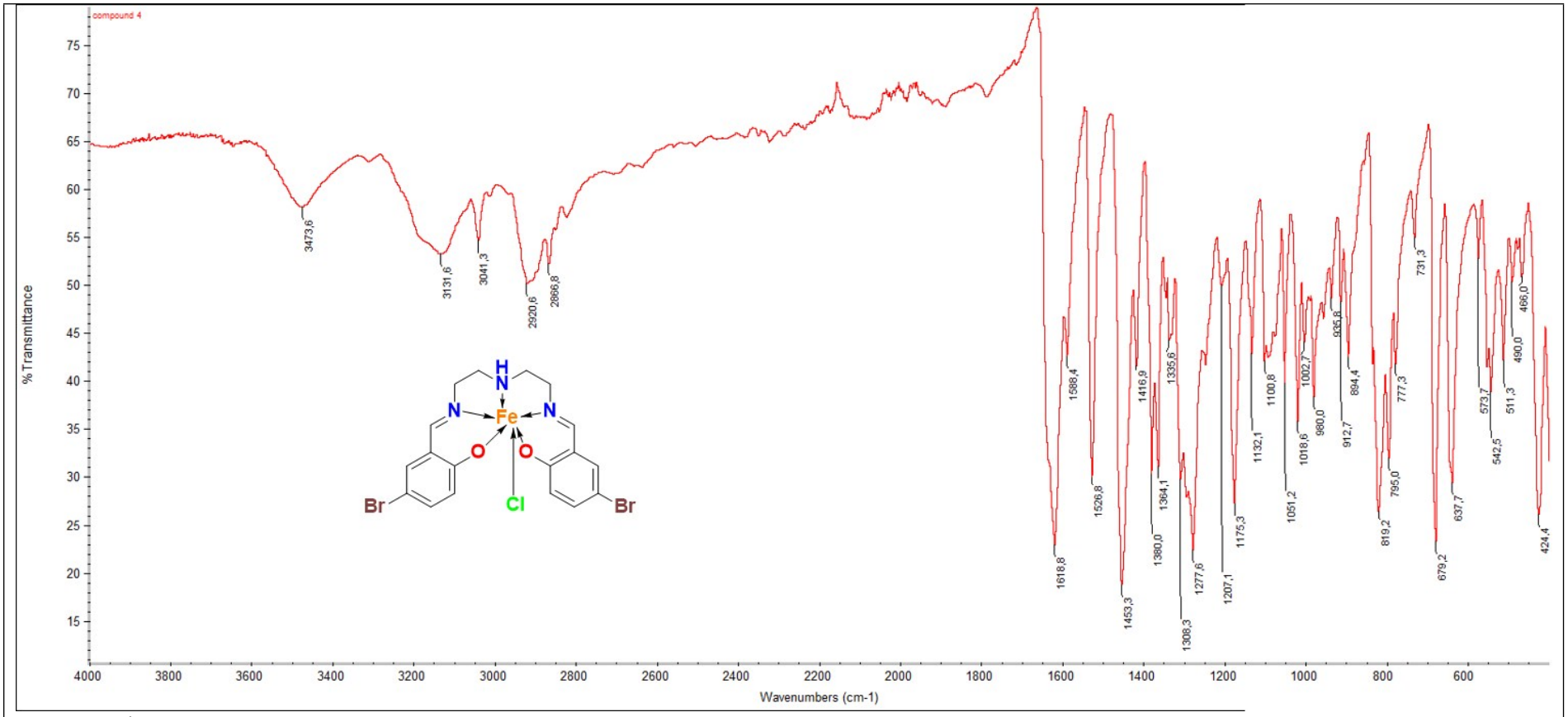
compound 4
% Transmittance
Wavenumbers (cm-1)
3473,6
3131,6
3041,3
2920,6
2866,8
1618,8
1588,4
1526,8
1453,3
1416,9
1380,0
1364,1
1335,6
1308,3
1277,6
1207,1
1175,3
1132,1
1100,8
1051,2
1018,6
1002,7
980,0
935,6
912,7
894,4
819,2
795,0
777,3
731,3
679,2
637,7
573,7
542,5
511,3
490,0
466,0
424,4
H
N
N
Fe
N
O
O
Br
Cl
Br

Compound **4**

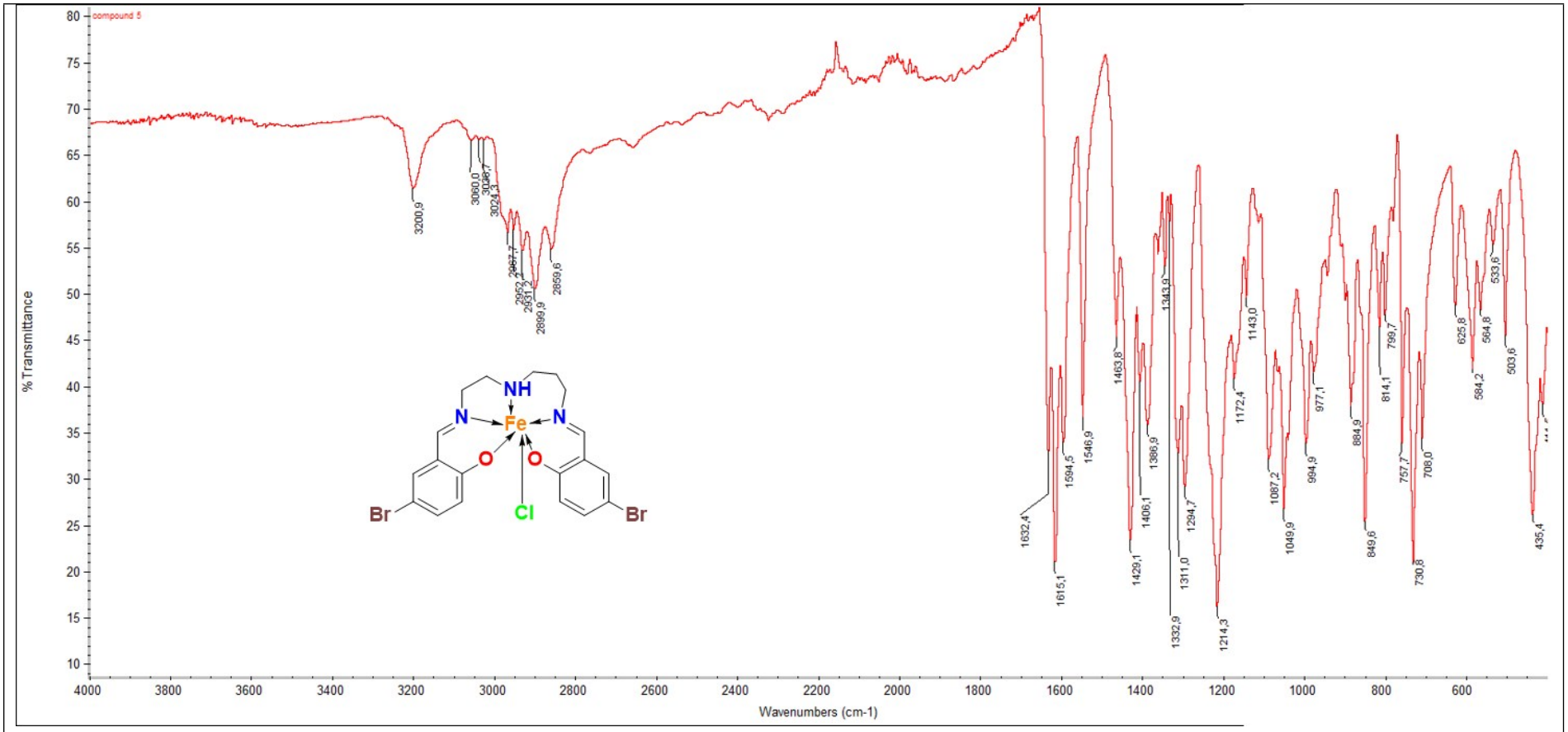
compound 5
% Transmittance
Wavenumbers (cm-1)
3200,9
3060,0
3048,7
3024,3
2967,7
2953,2
2931,1
2899,9
2859,6
1632,4
1615,1
1594,5
1546,9
1463,8
1429,1
1406,1
1386,9
1343,9
1332,9
1311,0
1294,7
1214,3
1172,4
1143,0
1087,2
1049,9
994,9
977,1
884,9
849,6
814,1
799,7
757,7
730,8
708,0
625,8
584,2
564,8
533,6
503,6
435,4
NH
N
Fe
N
O
O
Br
Cl
Br

Compound **5**

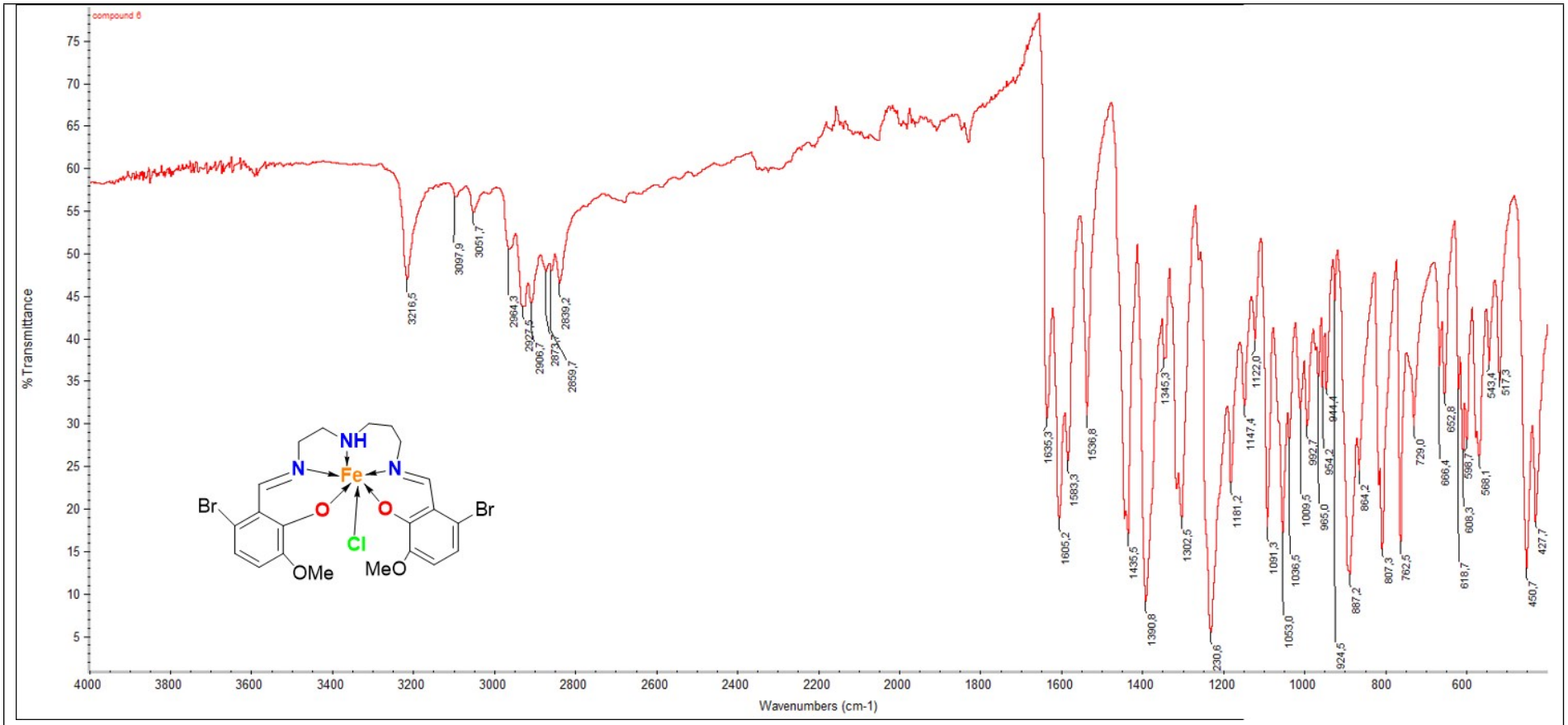
compound 6
% Transmittance
Wavenumbers (cm-1)
3216,5
3097,9
3051,7
2964,3
2927,5
2906,7
2873,7
2859,7
2839,2
1635,3
1605,2
1583,3
1536,8
1435,5
1390,8
1345,3
1302,5
1230,6
1181,2
1147,4
1122,0
1091,3
1053,0
1036,5
1009,5
992,7
965,0
954,2
944,4
924,5
887,2
864,2
807,3
762,5
729,0
666,4
652,8
618,7
608,3
598,7
568,1
543,4
517,3
450,7
427,7
NH
N
Fe
N
Br
O
O
Br
Cl
OMe
MeO

Compound **6**

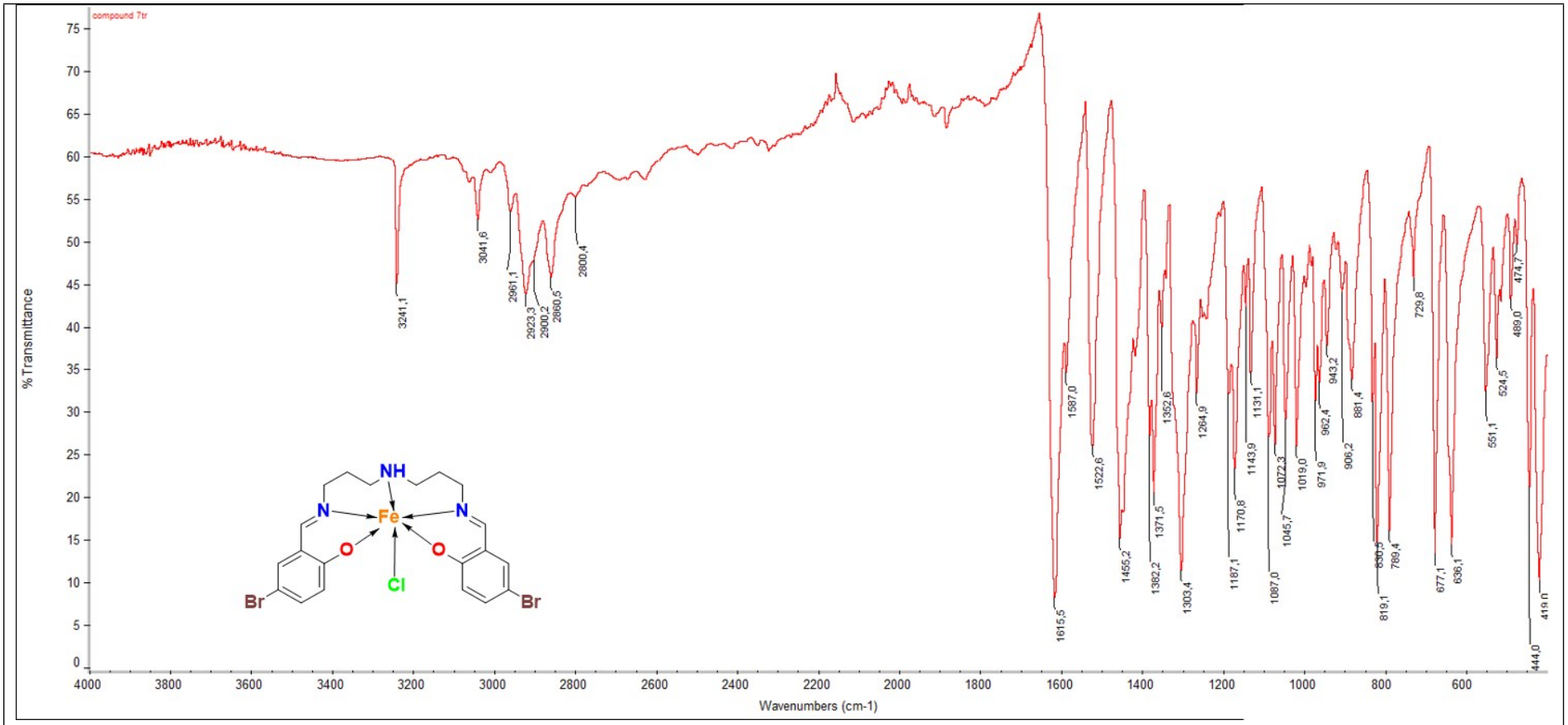
compound 7tr
% Transmittance
Wavenumbers (cm-1)
3241,1
3041,6
2961,1
2923,3
2900,2
2860,5
2800,4
1615,5
1587,0
1522,6
1455,2
1371,5
1352,6
1303,4
1264,9
1187,1
1170,8
1143,9
1131,1
1087,0
1072,3
1045,7
1019,0
971,9
962,4
943,2
906,2
881,4
819,1
830,5
789,4
729,8
677,1
636,1
551,1
524,5
489,0
474,7
444,0
419,0
NH
N
N
Fe
O
O
Cl
Br
Br

Compound **7t**

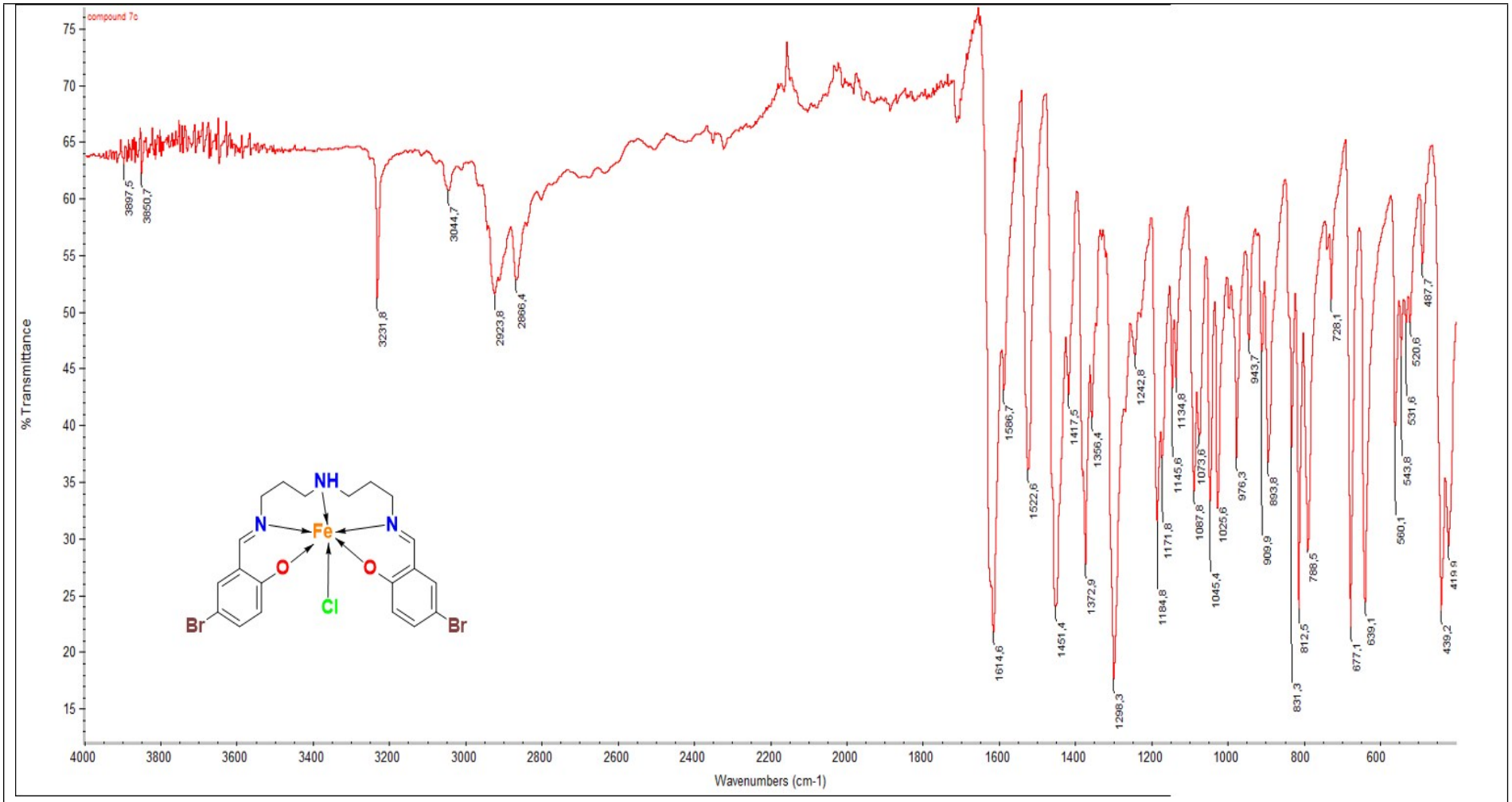
compound 7c
% Transmittance
Wavenumbers (cm-1)
3897,5
3850,7
3231,8
3044,7
2923,8
2866,4
1614,6
1586,7
1522,6
1451,4
1417,5
1372,9
1356,4
1298,3
1242,8
1184,8
1171,8
1145,6
1134,8
1087,8
1073,6
1045,4
1025,6
976,3
943,7
909,9
893,8
831,3
812,5
788,5
728,1
677,1
639,1
560,1
543,8
531,6
520,6
487,7
439,2
419,9
NH
N
N
Fe
O
O
Cl
Br
Br

Compound **7c**

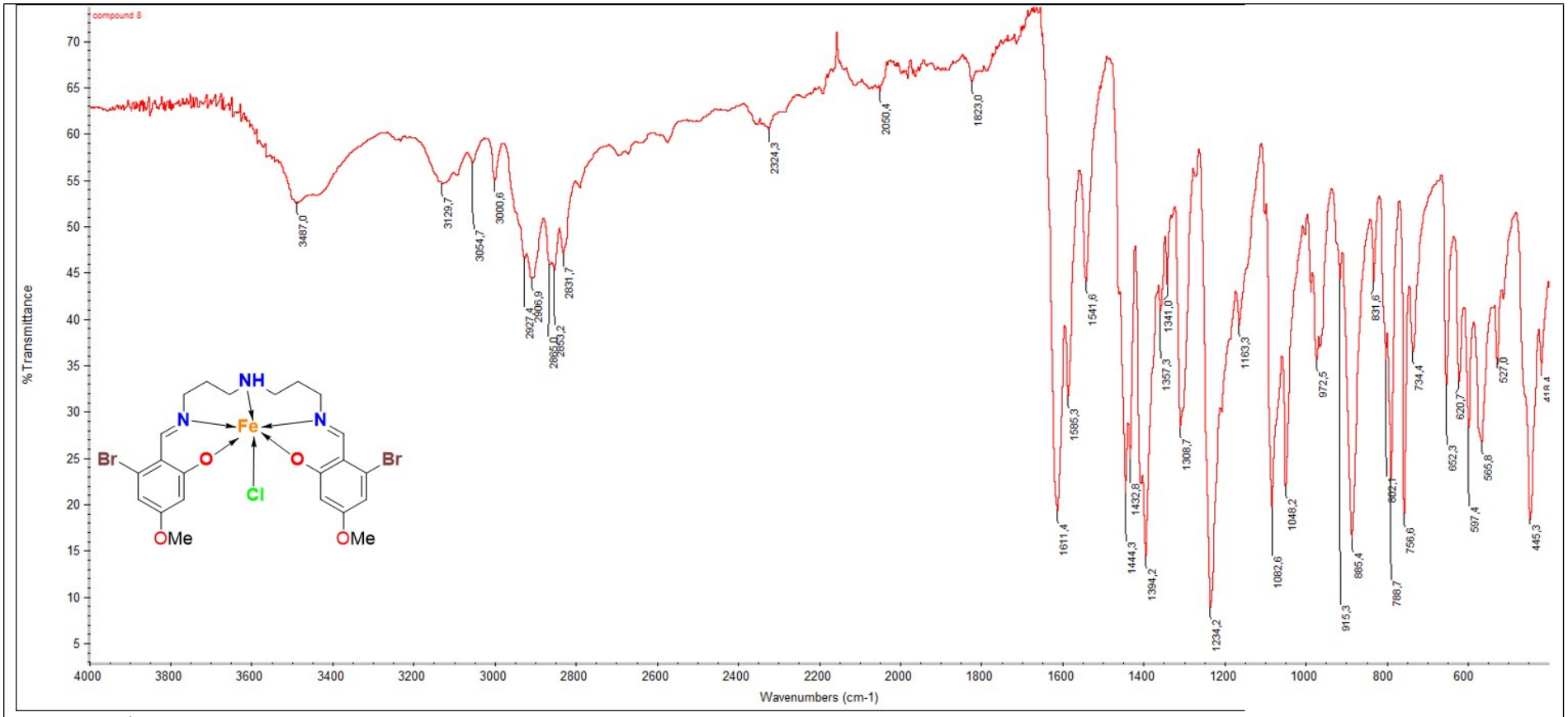
compound 8
% Transmittance
Wavenumbers (cm-1)
3487,0
3129,7
3054,7
3000,6
2927,4
2906,9
2885,0
2863,2
2831,7
2324,3
2050,4
1823,0
1611,4
1585,3
1541,6
1444,3
1432,8
1394,2
1357,3
1341,0
1308,7
1234,2
1163,3
1082,6
1048,2
972,5
915,3
885,4
831,6
802,1
788,7
756,6
734,4
652,3
620,7
597,4
565,8
527,0
445,3
NH
N
Fe
N
Br
O
O
Br
Cl
OMe
OMe

Compound **8**

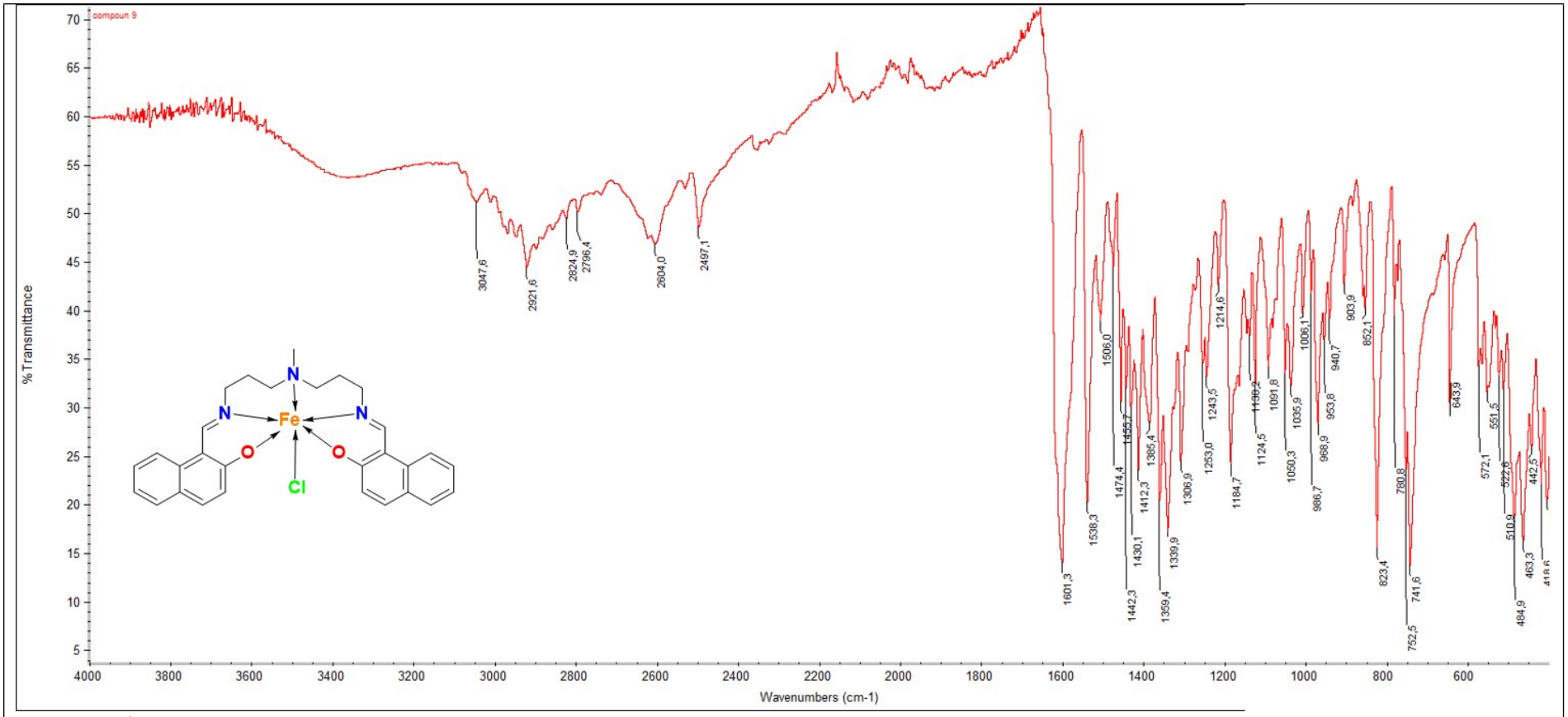
compoun 9
% Transmittance
Wavenumbers (cm-1)
3047,6
2921,6
2824,9
2796,4
2604,0
2497,1
1601,3
1538,3
1506,0
1474,4
1455,7
1442,3
1430,1
1412,3
1385,4
1359,4
1339,9
1306,9
1253,0
1243,5
1214,6
1184,7
1139,2
1124,5
1091,8
1050,3
1035,9
1006,1
986,7
966,9
953,8
940,7
903,9
852,1
823,4
780,8
752,5
741,6
643,9
572,1
551,5
522,6
510,9
484,9
463,3
442,5
N
N
N
Fe
O
O
Cl

Compound **9**

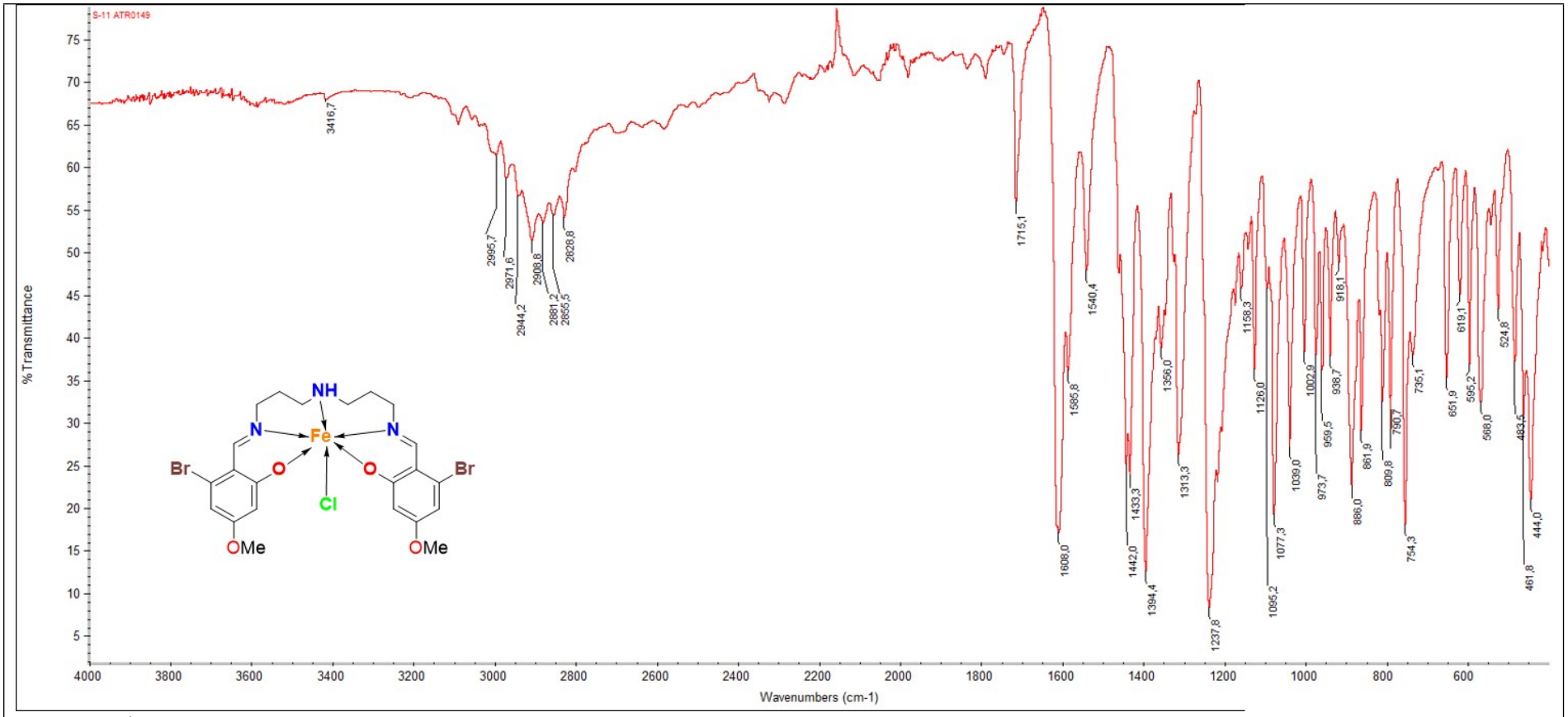
S-11 ATR0149
% Transmittance
Wavenumbers (cm-1)
3416,7
2995,7
2971,6
2944,2
2908,8
2881,2
2855,5
2828,8
1715,1
1608,0
1585,8
1540,4
1442,0
1433,3
1394,4
1356,0
1313,3
1237,8
1158,3
1126,0
1095,2
1077,3
1039,0
1002,9
973,7
959,5
938,7
918,1
886,0
861,9
809,8
790,7
754,3
735,1
651,9
619,1
595,2
568,0
524,8
483,5
461,8
444,0
NH
N
N
Fe
Cl
O
O
Br
Br
OMe
OMe

Compound **10**

S3. Supplementary crystallographic information

Table S3.1 Bond distances and angles of coordination polyhedra for **1** – **10**

Complex **1**	Complex **2**	Complex **3**
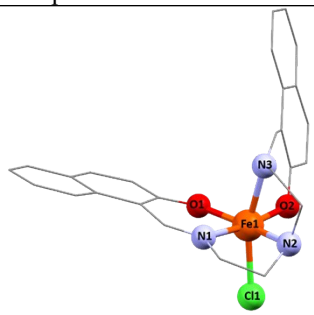 **At 293 K: bond distances (in Å)** Fe1-O1=1.926(2) Fe1-O2=1.970(2) Fe1-N1=2.139(2) Fe1-N2=2.235(2) Fe1-N3=2.102(15) Fe1- Cl1=2.3217(8) **bond angles (in °)** cis O2-Fe1-N3=83.03(8) N2-Fe1-N3=76.61(8) N1-Fe1-N3=89.95(9) O1-Fe1-N3=96.92(6) O2-Fe1-N2 = 106.22(8) N2-Fe1-N1=75.68(8) N1-Fe1-O1=84.63(8) O1-Fe1-O2=92.62(5) O2-Fe1-Cl1=92.42(8) N2-Fe1-Cl1=87.89(6) N1-Fe1-Cl1=95.63(6) O1-Fe1-Cl1=100.60(6) trans O2-Fe1-N1= 172.00(8) N2-Fe1-O1= 159.27(8) N3-Fe1-Cl1= 161.71(7) **Σ=87° Θ=211°**	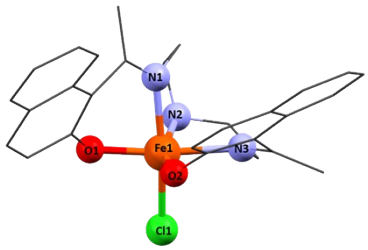 **At 100 K: bond distances (in Å)** Fe1-O1=1.960(2) Fe1-O2=1.934(2) Fe1-N1=2.153(3) Fe1-N2=2.208(2) Fe1-N3=2.163(2) Fe1-Cl1=2.3236(8) **bond angles (in °)** cis O1-Fe1-N1=81.56(7) N2-Fe1-N1=78.84(8) N3-Fe1-N1=91.82(8) O2-Fe1-N1=93.34(7) O1-Fe1-N2 = 103.73(7) N2-Fe1-N3=76.29(7) N3-Fe1-O2=83.73(7) O2-Fe1-O1=95.08(7) O1-Fe1-Cl1 = 94.49(5) N2-Fe1-Cl1=90.43(5) N3-Fe1-Cl1 = 92.30(6) O2-Fe1-Cl1=99.11(5) trans O2-Fe1-N2= 158.20(7) N3-Fe1-O1= 159.27(8) N1-Fe1-Cl1= 173.21(7) **Σ=80° Θ=181°**	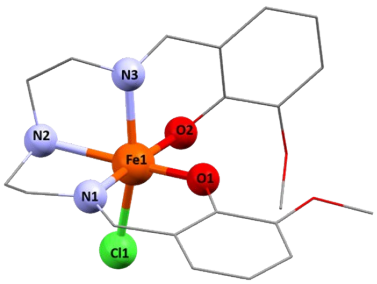 **At 293 K: bond distances (in Å):** Fe1-O1=1.915(3) Fe1-O2=1.941(2) Fe1-N1 = 2.153(3) Fe1-N2=2.226(3) Fe1-N3=2.132(4) Fe1- Cl1=2.329(2) **bond angles (in °)** cis O1-Fe1-N3=95.4(1) N1-Fe1-N3=96.0(1) N2-Fe1-N3=75.7(1) O2-Fe1-N3=82.4(1) O1-Fe1-N1=84.5(1) N1-Fe1-N2=75.9(1) N2-Fe1-O2=110.3(1) O2-Fe1-O1=88.6(1) O1-Fe1-Cl1=102.95(9) N1-Fe1-Cl1=92.26(9) N2-Fe1-Cl1=89.30(9) O2-Fe1-Cl1=91.51(8) trans O1-Fe1-N2= 157.4(1) N1-Fe1-O2= 172.8(1) N3-Fe1-Cl1= 160.5(1) **Σ=92° Θ=249°**
Complex **4**		

At 150 K: **bond distances (in Å):** Fe1-O1 =1.923(1) Fe1-O2=1.956(2) Fe1-N1 =2.170(2) Fe1-N2 = 2.201(2) Fe1-N3 = 2.125(2) Fe1- Cl1=2.3104(7) **bond angles (in °)** cis O1-Fe1-N3=97.03(8) N1-Fe1-N3=90.45(8) N2-Fe1-N3 = 76.42(8) O2-Fe1-N3 = 82.48(8) O1-Fe1-N1 = 84.77(8) N1-Fe1-N2 = 76.66(8) N2-Fe1-O2 =111.54(7) O2-Fe1-O1 = 85.68(7) O1-Fe1-Cl1 = 99.55(6) N1-Fe1-Cl1 = 95.44(6) N2-Fe1-Cl1 = 89.24(6) O2-Fe1-Cl1 = 94.33(5) trans O1-Fe1-N2=160.16(8) N1-Fe1-O2=167.34(8) N3-Fe1-Cl1=162.83(6) **Σ=93° Θ=231°**	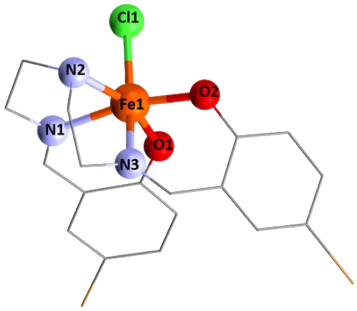 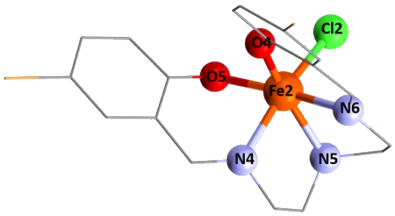	**At 150 K:** **bond distances (in Å)** Fe2-O3=1.961(2) Fe2-O4=1.929(2) Fe2-N4=2.131(2) Fe2-N5=2.202(2) Fe2-N6 = 2.171(2) Fe2- Cl2=2.3097(7) **bond angles (in°)** cis O4-Fe2-N4=96.75(8) N6-Fe2-N4 = 88.46(8) N5-Fe2-N4 =76.25(8) O3-Fe2-N4 = 83.28(8) O4-Fe2-N6 = 84.57(8) N6-Fe2-N5 = 76.07(8) N5-Fe2-O3=110.42(8) O3-Fe2-O4 = 87.47(8) O4-Fe2-Cl2 = 99.40(6) N6-Fe2-Cl2 = 96.61(6) N5-Fe2-Cl2=89.66(6) O3-Fe2-Cl2 = 93.81(5) trans O3-Fe1-N6=167.78(8) N5-Fe1-O4=159.47(8) N4-Fe1-Cl2=163.46(6) **Σ=92° Θ=221°**

Complex **5(P-1)**		Complex **5(P2$_1$/c)**	Complex **6**
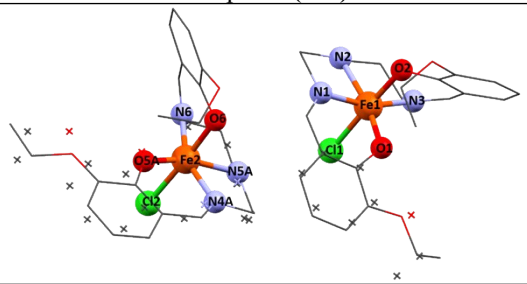		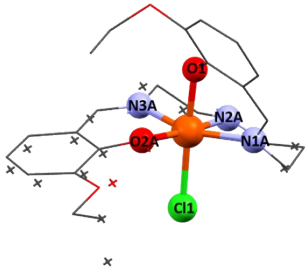	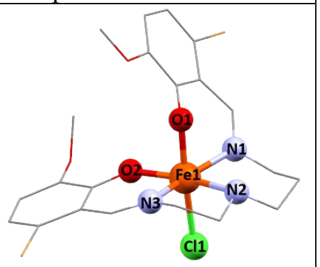
At 150 K: bond distances (in Å) Fe1-O1=1.914(2) Fe1-O2=1.969(2) Fe1-N1=2.086(3) Fe1-N2=2.196(3) Fe1-N3=2.108(2) Fe1-Cl1=2.403(1) **bond angles (in °)** cis N1-Fe1-N2=78.8(1) N2-Fe1-Cl1=87.96(8) Cl1-Fe1-N1=93.16(8) O1-Fe1-Cl1=89.53(7) N3-Fe1-Cl1=93.19(8) O2-Fe1-N1=89.9(1) O2-Fe1-O1=90.55(9) O2-Fe1-N3=83.85(9) O2-Fe1-N2=92.7(1) N1-Fe1-O1=88.4(1) O1-Fe1-N3=108.2(1) N3-Fe1-N2=84.9(1) N2-Fe1-N1=78.8(1) trans O1-Fe1-N2= 166.8(1) N1-Fe1-N3= 162.3(1) O2-Fe1-Cl1=176.91(6) **Σ=54° Θ=159°**	**At 150 K: bond distances (in Å)** Fe2-O5A= 1.819(2) Fe2-O5B= 1.962(1) Fe2-O6= 1.973(2) Fe2-N4A= 2.033(2) Fe2-N4B= 2.156(2) Fe2-N5A= 2.288(2) Fe2-N5B= 2.152(2) Fe2-N6= 2.111(2) Fe2- Cl2= 2.391(1) **bond angles (in °)** cis O6-Fe2-N6=83.76(8) O6-Fe2-N5A=93.50(8) O6-Fe2-N4A=88.82(8) O6-Fe2-O5A=95.12(8) O5A-Fe2-N4A=92.78(8) N4A-Fe2-N5A=77.18(8) N5A-Fe2-N6=77.50(8) N6-Fe2-O5A=113.59(8) O5A-Fe2-Cl2=84.53(6) N6-Fe2-Cl2=92.97(6) N5A-Fe2-Cl2=87.53(6) N4A-Fe2-Cl2=94.90(6) O6-Fe2-N5B=94.09(8) O6-Fe2-N4B=90.04(8) O6-Fe2-O5B=87.77(7) N6-Fe2-O5B=106.87(7) O5B-Fe2-N4B=84.71(7) N4B-Fe2-N5B=77.96(8) N5B-Fe2-N6=90.57(8) N5B-Fe2-Cl2=87.73(6) N4B-Fe2-Cl2=93.52(6) O5B-Fe2-Cl2=91.47(5) trans N6-Fe2-N4A=153.08(8) N6-Fe2-N4B=166.57(8) Cl2-Fe2-O6=176.27(6) O5A-Fe2-N5A=166.63(8) N5B-Fe2-O5B=162.56(8) **Σ(A)=84° Θ(A)=213°** **Σ(B)=58° Θ(B)=167°**	**At 293 K: bond distances (in Å)**: Fe1-O1=1.968(2) Fe1-O2=1.92(1) Fe1-O2A=1.921(6) Fe1-N1=2.108(2) Fe1-N1A=2.1083(19) Fe1-N2=2.21(1) Fe1-N2A=2.208(6) Fe1-N3=2.10(1) Fe1-N3A=2.100(6) Fe1-Cl1=2.3997(9) **bond angles (in °):** cis O1-Fe1-N2=94.9(4) O1-Fe1-N1=83.72(7) O1-Fe1-O2=87.5(5) O1-Fe1-N3=88.0(4) N1-Fe1-N2=79.7(4) N2-Fe1-N3=77.1(6) N3-Fe1-O2=90.2(6) O2-Fe1-N1=113.4(5) Cl1-Fe1-N1=93.39(6) Cl1-Fe1-N2=85.8(4) Cl1-Fe1-N3=95.1(4) O2-Fe1-Cl1=92.5(5) Cl1-Fe1-N1A=93.39(5) Cl1-Fe1-N2A=88.9(2) Cl1-Fe1-N3A=93.0(2) Cl1-Fe1-O2A=87.5(2) N3A-Fe1-O1=90.1(2) O2A-Fe1-O1=92.2(2) O1-Fe1-N1A=83.71(6) O1-Fe1-N2A=92.2(2) N2A-Fe1-N3A=79.4(3) N3A-Fe1-O2A=87.3(3) O2A-Fe1-N1A=106.9(2) N1A-Fe1-N2A=86.81(19) trans N3-Fe1- N1=154.6(3) O2-Fe1-N2=167.0(6) O1-Fe1-Cl1=176.85(5) N3A-Fe1-N1A=164.60(17) O2A-Fe1-N2A=166.0(3) **Σ=78° Θ=199°** **Σ(A)=54° Θ(A)=199°**	**At 293 K: bond distances (in Å)** Fe1-O1=1.945(3) Fe1-O2=1.924(3) Fe1-N1 = 2.122(3) Fe1-N2=2.193(3) Fe1-N3 = 2.092(3) Fe1- Cl1=2.354(2) **bond angles (in °)** cis N1-Fe1-O1=81.9(1) N2-Fe1-O1=90.0(1) N3-Fe1-O1=90.6(1) O2-Fe1-O1=90.5(1) N1-Fe1-N2=85.1(1) N2-Fe1-N3=78.4(1) N3-Fe1-O2=86.8(1) O2-Fe1-N1=109.5(1) N1-Fe1-Cl1=93.53(9) N2-Fe1-Cl1=89.9(1) N3-Fe1-Cl1=93.91(9) O2-Fe1-Cl1=90.82(8) trans O2-Fe1-N2= 165.2(1) N3-Fe1-N1=161.9(1) O1-Fe1-Cl1= 175.38(9) **Σ=57° Θ=169°**

Complex **7t**	Complex **7c**
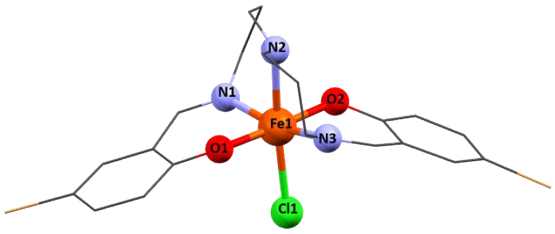 **At 150 K:** **bond distances (in Å):** Fe1-O1=1.916(5) Fe1-O2=1.936(5) Fe1-N1=2.056(7)) Fe1-N2=2.200(6) Fe1-N3=2.070(7)) Fe1-Cl1=2.396(2) **bond angles (in °):** cis O1-Fe1-N2=90.7(2) N1-Fe1-N2=86.8(3) O2-Fe1-N2=87.4(2) N3-Fe1-N2=79.1(3) O1-Fe1-N1=87.6(2) N1-Fe1-O2=91.5(2) O2-Fe1-N3=88.6(2) N3-Fe1-O1=91.8(2) O1-Fe1-Cl1=90.1(2) N1-Fe1-Cl1=99.4(2) O2-Fe1-Cl1=91.8(2) N3-Fe1-Cl1 = 94.8(2) trans O1-Fe1-O2= 178.0(2) N3-Fe1-N1= 165.8(3) N2-Fe1-Cl1= 173.8(2) **Σ=41° Θ=105°**	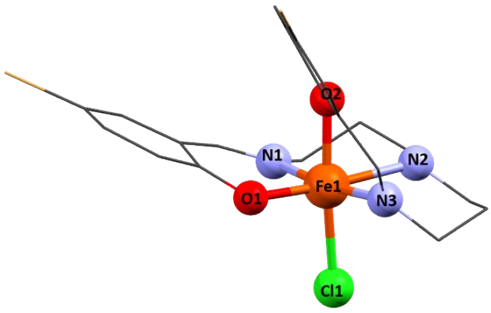 **At 293 K:** **bond distances (in Å):** Fe1-O1=1.938(2) Fe1- N1=2.113(2) Fe1- N2=2.253(2) Fe1- N3=2.111(3) Fe1- O2=1.960(2) Fe1- Cl1=2.327(1) **bond angles (in °):** cis O1-Fe1-O2=89.13(9) N1-Fe1-O2= 90.00(9) N2-Fe1-O2= 85.52(9) N3-Fe1-O2= 84.21(9) O1-Fe1-N1= 89.50(9) N1-Fe1-N2= 92.00(9) N2-Fe1-N3= 83.52(9) N3-Fe1-O1= 94.5(1) O1-Fe1-Cl1= 95.03(7) N1-Fe1-Cl1= 91.38(7) N2-Fe1-Cl1= 90.28(7) N3-Fe1-Cl1= 94.11(7) trans O1-Fe1-N2= 174.4(1) N3-Fe1-N1= 172.9(1) O2-Fe1-Cl1=175.63(7) **Σ=36° Θ=52°**
Complex **8**	Complex **9**
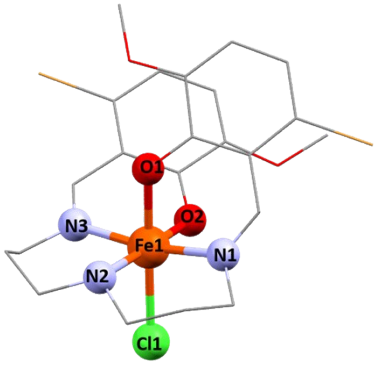 **At 293 K: bond distances (in Å):** Fe4-O1=1.978(6) Fe4-O2=1.931(5) Fe4-N1=2.118(7) Fe4-N2=2.203(7)	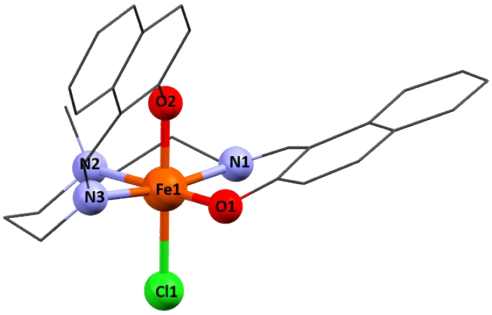 **At 293 K: bond distances (in Å):** Fe1-O1 = 1.918(3) Fe1-O2 = 1.963(3) Fe1-N1 = 2.099(3) Fe1-N2 = 2.300(3)

Fe4-N3=2.090(7) Fe4- Cl1 = 2.342(3) **bond angles (in °):** cis N1-Fe4-O1=81.8(3), N2-Fe4-O1=88.9(3) N3-Fe4-O1=87.9(9) O2-Fe4-O1 = 91.2(2) N1-Fe4-N2 = 86.6(3) N2-Fe4-N3=93.1(3) N3-Fe4-O2 = 85.5(3) O2-Fe4-N1=94.7(3) N1-Fe4-Cl1 = 95.7(2) N2-Fe4-Cl1=89.1(2) N3-Fe4-Cl1 = 94.5(2) O2-Fe4-Cl1 = 90.8(2) trans N2-Fe1-O2= 178.7(3) N3-Fe1-N1= 169.8(3) O1-Fe1-Cl1= 177.0(2) **Σ=40° Θ=86°**	Fe1-N3 = 2.092(3) Fe1- Cl1 = 2.362(1) **bond angles (in °)** cis N3-Fe1-O2 = 85.0(1) N2-Fe1-O2 = 91.0(1) N1-Fe1-O2 = 85.9(1) O1-Fe1-O2 = 89.0(1) N3-Fe1-N2=83.5(1) N2-Fe1-N1 = 93.7(1) N1-Fe1-O1 = 87.7(1) O1-Fe1-N3 = 95.2(1) N3-Fe1-Cl1 = 96.41(9) N2-Fe1-Cl1 = 87.66(8) N1-Fe1-Cl1 = 92.52(9) O1-Fe1-Cl1 = 92.35(8) trans N2-Fe1-O1= 177.91(9) N3-Fe1-N1= 170.5(1) O2-Fe1-Cl1= 177.91(9) **Σ=42° Θ=86°**

Compound **10**

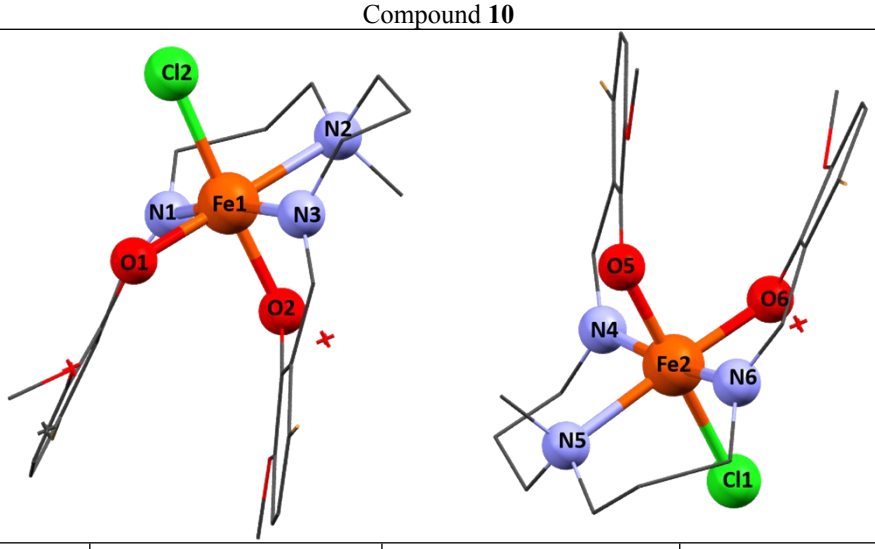

At 100 K: **bond distances (in Å)** Fe1-O1=1.936(1) Fe1-O2=1.996(1) Fe1-N1=2.096(1) Fe1-N2=2.250(1) Fe1-N3=2.120(2) Fe1-Cl2=2.3358(5) **bond angles (in °)** cis N3-Fe1-O1=93.33(6) N3-Fe1-Cl2=97.13(5) N3-Fe1-N2=87.58(6) N3-Fe1-O2=81.86(6) O2-Fe1-O1=90.70(5) O1-Fe1-Cl2=91.86(4) Cl2-Fe1-N2=87.99(4) N2-Fe1-O2=89.46(5) O1-Fe1-N1=86.37(6) O2-Fe1-N1=85.73(5) N2-Fe1-N1=92.75(6)	**At 293 K: bond distances (in Å)** O1-Fe1=1.929(2) O2-Fe1=1.984(2) N1-Fe1=2.094(2) N2-Fe1=2.265(2) N3-Fe1=2.112(2) Cl2-Fe1=2.3286(9) **Bond angles (in °)** cis N1-Fe1-O1=86.51(8) N1-Fe1-O2=85.97(8) N1-Fe1-N2=92.17(9) N1-Fe1-Cl2=95.22(7) N3-Fe1-Cl2=96.52(7) N3-Fe1-O1=94.33(8) N3-Fe1-O2=82.25(8) N3-Fe1-N2=86.98(9) N2-Fe1-Cl2=88.29(6) Cl2-Fe1-O1=91.77(7) N2-Fe1-O2=89.42(8)	**At 100 K:** **bond distances (in Å)** Fe2-O5=1.967(1) Fe2-O6=1.948(1) Fe2-N4=2.100 (2) Fe2-N5 = 2.255(2) Fe2-N6 = 2.1139(17) Fe2- Cl1=2.3644(5) **bond angles (in°)**: cis N6-Fe2-Cl1=95.83(5) N6-Fe2-N5=92.47(6) N6-Fe2-O5=87.43(6) N6-Fe2-O6=84.61(6) O6-Fe2-O5=90.83(6) O5-Fe2-N5=90.43(6) N5-Fe2-Cl1=89.99(5) Cl1-Fe2-O6=88.93(4) O6-Fe2-N4=94.44(6) O5-Fe2-N4=82.99(6) N5-Fe2-N4=88.67(6)	**At 293 K: bond distances (in Å)** O5-Fe2=1.961(1) O6-Fe2=1.944(2) N4-Fe2=2.091(2) N5-Fe2=2.255(2) N6-Fe2=2.112(2) Cl1-Fe2=2.3612(8) **bond angles (in °)** cis O5-Fe2-N5=90.62(8) O5-Fe2-N4=83.31(8) O5-Fe2-O6=90.71(8) O5-Fe2-N6=86.94(6) N4-Fe2-Cl1=94.21(7) O6-Fe2-Cl1=88.98(6) N6-Fe2-Cl1=95.54(7) N5-Fe2-Cl1=89.82(6) N5-Fe2-N6=92.51(9) N6-Fe2-O6=84.55(8) N5-Fe2-N4=87.91(7)

Cl2-Fe1-N1=95.29(4) trans N2-Fe1-O1=178.67(8) N3-Fe1-N1=168.19(9) O2-Fe1-Cl2=177.46(6) **Σ=43° Θ=93°**	O2-Fe1-O1=90.54(8) trans N2-Fe1-O1= 179.09(6) N3-Fe1-N1= 167.58(6) O2-Fe1-Cl2= 177.30(4) **Σ=41° Θ=88°**	Cl1-Fe2-N4=93.74(5) trans N5-Fe1-O6= 176.70(8) N4-Fe1-N6= 170.24(9) O5-Fe1-Cl1= 177.47(6) **Σ=37° Θ=93°**	O6-Fe2-N4=95.25(8) trans N5-Fe1-O6= 176.77(6) N4-Fe1-N6=170.36(6) O5-Fe1-Cl1= 176.69(4) **Σ=37° Θ=92°**

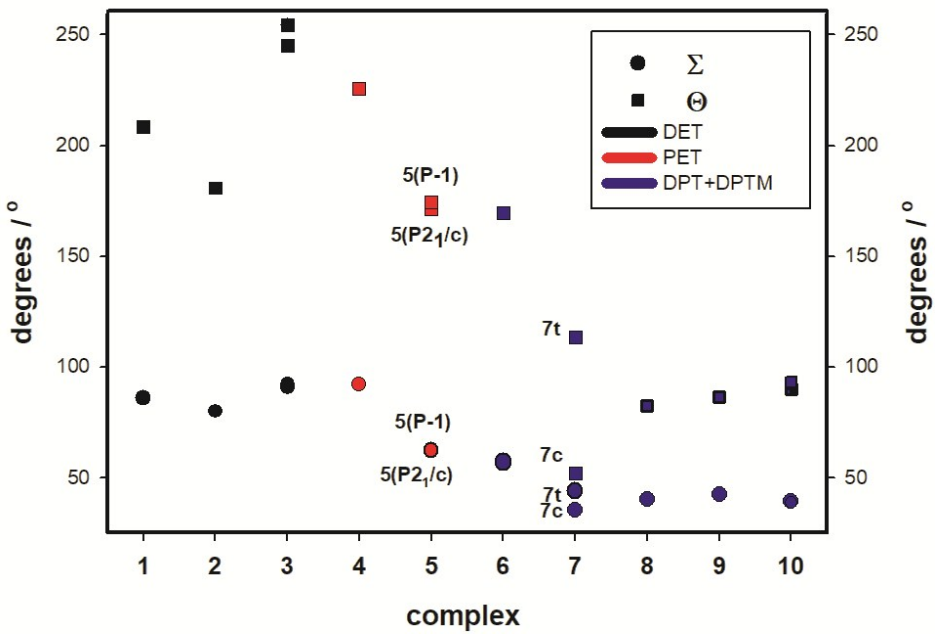
Σ
Θ
DET
PET
DPT+DPTM
5(P-1)
5(P2$_1$/c)
7t
7c
degrees / °
complex

a)

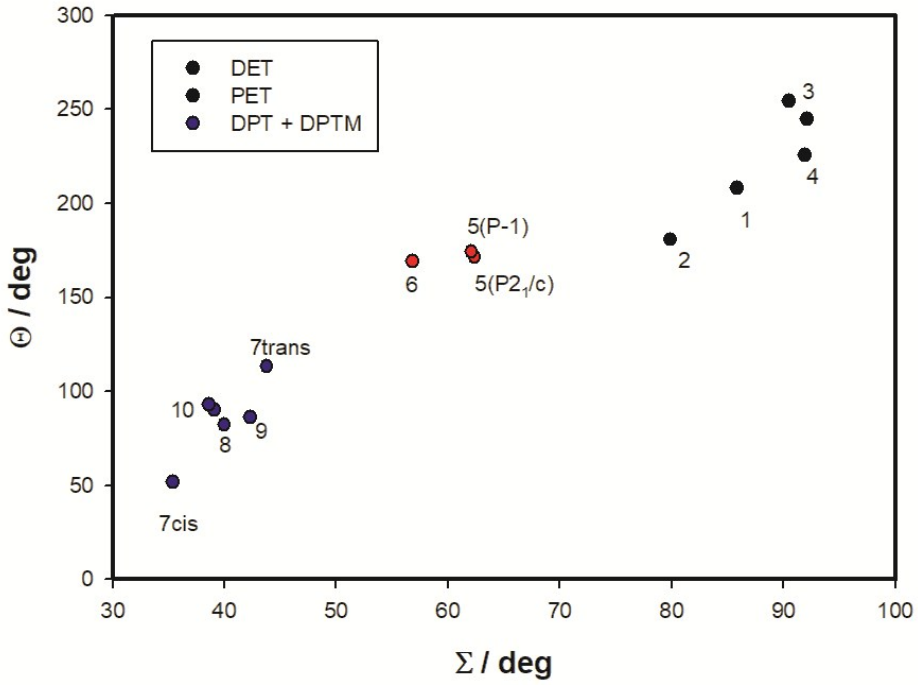
DET
PET
DPT + DPTM
5(P-1)
5(P2$_1$/c)
7trans
7cis
Θ / deg
Σ / deg

b)

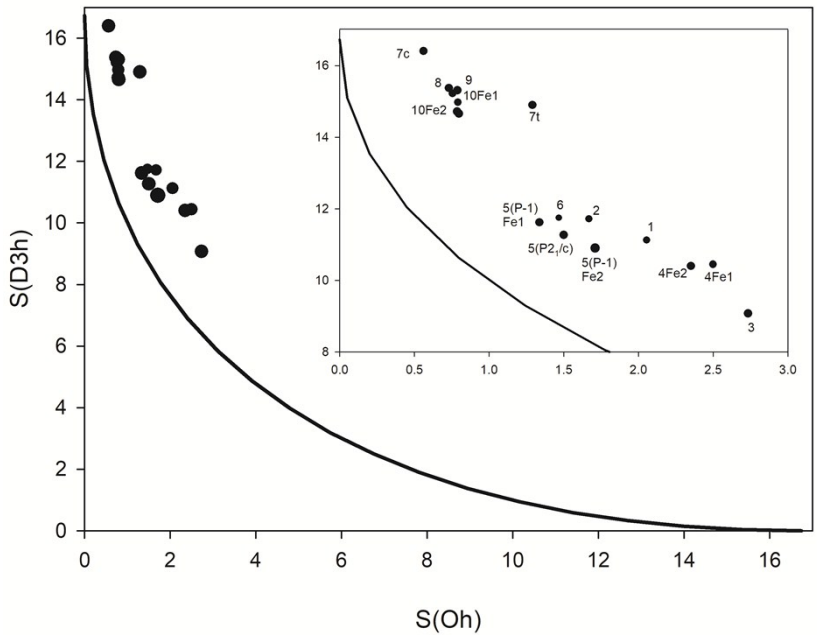

c)

Figure S3.1 a) Plotted Σ and Θ distortion parameters for reported compounds and ***b)*** their mutual correlation. c) Symmetry measure parameters for 1-11. Solid line represents ideal Bailar-type trigonal twist from octahedron (O_h) and trigonal prism (D_{3h}) geometry.

Table S3.2 Symmetry measure parameters of the reported compounds **1-10** calculated for hexagon (*D6h*), pentagonal pyramid (C5v), octahedron (Oh), trigonal prism (D3h) and Johnson pentagonal pyramid (C5v-J) symmetry

Complex	*D6h*	*C5v*	*Oh*	*D3h*	*C5v-J*
1	31.184	21.671	2.055	11.129	26.83
2	30.863	23.033	1.668	11.717	27.141
3	30.094	20.002	2.733	9.076	25.135
4 Fe1	29.911	20.501	2.499	10.448	25.644
4 Fe2	30.428	21.123	2.351	10.401	26.307
5(P-1) Fe1	32.116	24.292	1.337	11.62	28.193
5(P-1) Fe2A	32.818	22.313	2.063	10.151	25.549
5(P-1) Fe2B	32.027	23.901	1.376	11.597	28.893
5(P2$_1$/c) A	31.206	22.572	1.98	10.275	25.927
5(P2$_1$/c) B	32.628	24.652	1.242	11.803	28.746
6	32.133	23.636	1.467	11.749	28.698
7t A	33.13	26.371	1.193	14.693	29.153
7t B	30.447	26.318	1.671	15.737	29.976
7c	31.45	28.783	0.561	16.406	32.514
8	31.641	27.355	0.731	15.375	31.071
9	30.899	26.931	0.788	15.31	30.33
10 100K Fe1	31.817	26.881	0.791	14.974	30.626
10 100K Fe2	32.527	26.964	0.786	14.717	30.813
10 293 K Fe1	31.825	27.197	0.755	15.223	30.887
10 293 K Fe2	32.296	27.038	0.798	14.658	30.868

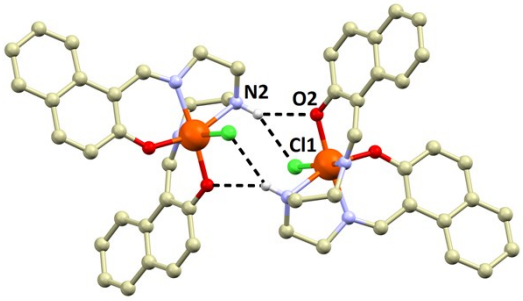

1

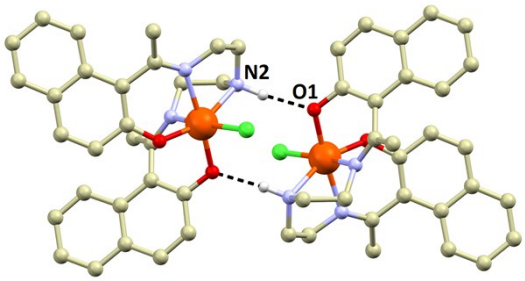

2

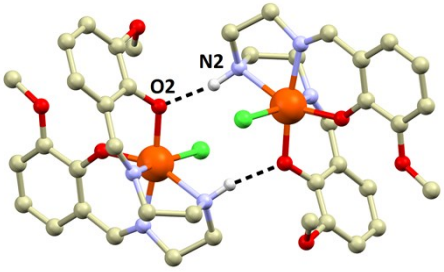

3

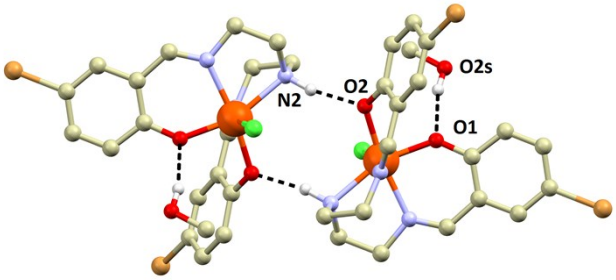

4

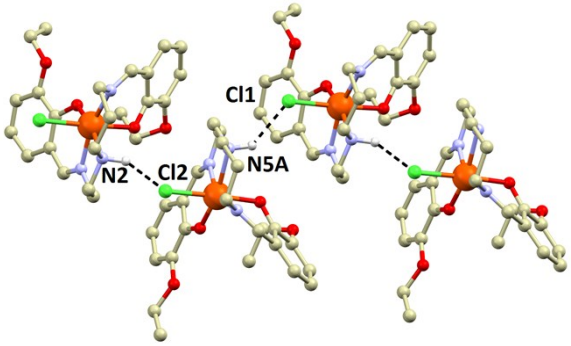

5(P-1)

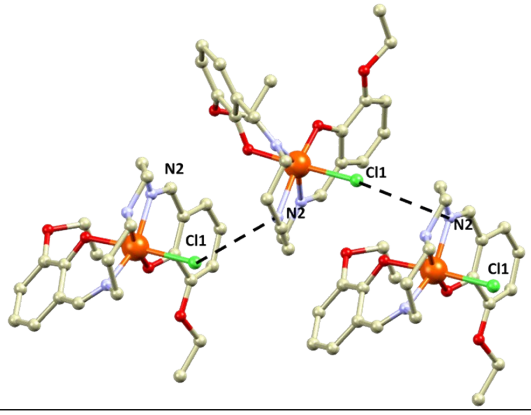

5(P2$_1$/c)

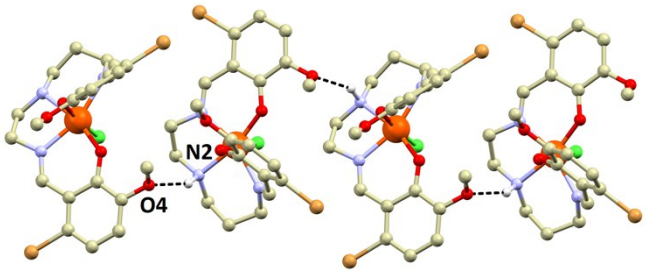

6

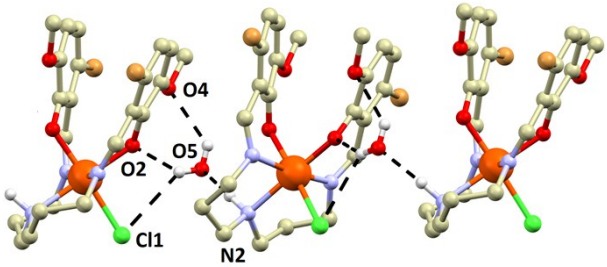

8

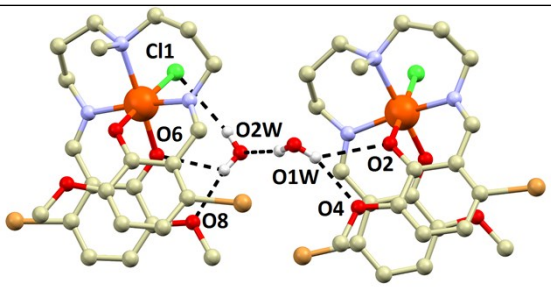

10

Figure S3.2 A perspective view on hydrogen bonds (dashed lines) in the compounds from presented series. Hydrogen atoms were omitted due to clarity (except of those involved in hydrogen bonding).

Table S3.3 Hydrogen bond geometry

contact	D···A/Å	D-H···A/°	H···A/Å	Symmetry codes
1_100K				
N2-H2···O2	3.245(3)	148.3	2.35	1-x,1-y,1-z
N2-H2···Cl1	3.474(2)	135.6	2.69	1-x,1-y,1-z
2_100K				
N2-H2···O1	3.003(2)	162.9	2.03	1-x,2-y,-z
3_293K				
N2-H2···O2	2.906(4)	164.1	1.95	1-x,1-y,1-z
4_150K				
O1S-H1S···O4	2.963(3)	163.6	2.15	x,y,z
N2-H2···O2	2.844(2)	168.6	1.86	1-x,1-y,-z
O2S-H2S···O1	2.967(3)	166.2	2.14	x,y,z
N5-H5A···O3	2.846(3)	163.8	1.87	-x,-y,1-z
5_150K				
N2-H2···Cl2	3.345(2)	134.8	2.56	x,1+y,z
N5A-H5A···Cl1	3.250(3)	137.1	2.45	x,y,z
N5B-H5B···Cl1	3.359(2)	141.1	2.52	x,y,z
5_293K				
N2A-H2A···Cl1	3.357(7)	139.1	2.55	x,1/2-y,1/2+z
N2-H2···Cl1	3.371(14)	135.2	2.60	x,1/2-y,1/2+z
6_293K				
N2-H2···O4	3.061(4)	152	2.26	-1/2+x,1/2-y,-1/2+z
8				
N2-H2···O5	2.957(11)	159.3	2.02	x,y,z
O5-H5A···O2	2.889(9)	143.9	2.19	x-1/2,-y+1/2,+z-1/2
O5-H5B···O4	2.973(10)	131.2	2.37	x-1/2,-y+1/2,+z-1/2
10				
O1W-H1WA···O2W	2.940(8)	167.7	2.11	-x+1,-y+1,-z+1
O1W-H1WB···O4	3.010(8)	156.5	2.22	x,y,z
O2W-H2WA···Cl1	3.556(6)	169.5	2.72	x,y,z
O2W-H2WB···O6	2.915(6)	121.7	2.38	x,y,z
O2W-H2WB···O8	3.010(8)	156.5	2.22	x,y,z

S4. Supplementary magnetic information

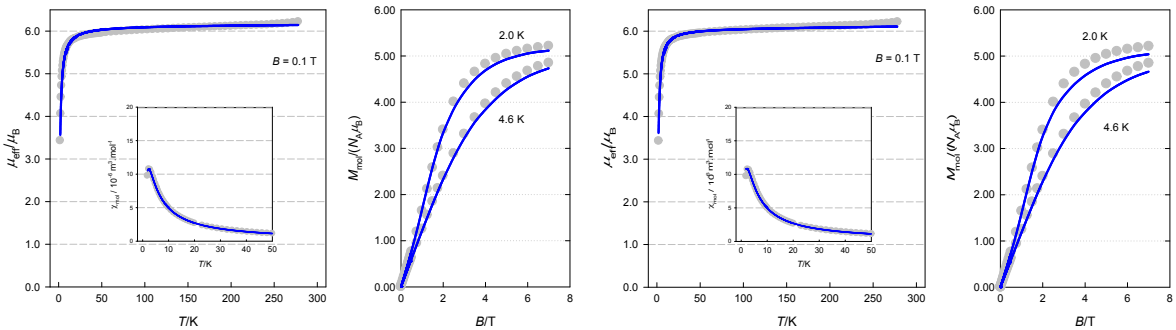

Figure S4.1 Magnetic functions for **1** (left two frames: alternative with negative D, right frames: positive D): effective magnetic moment *vs* temperature (left), magnetization *vs* magnetic field (right), magnetic susceptibility *vs* temperature (inset); grey circles: experimental data, solid line: fitted.

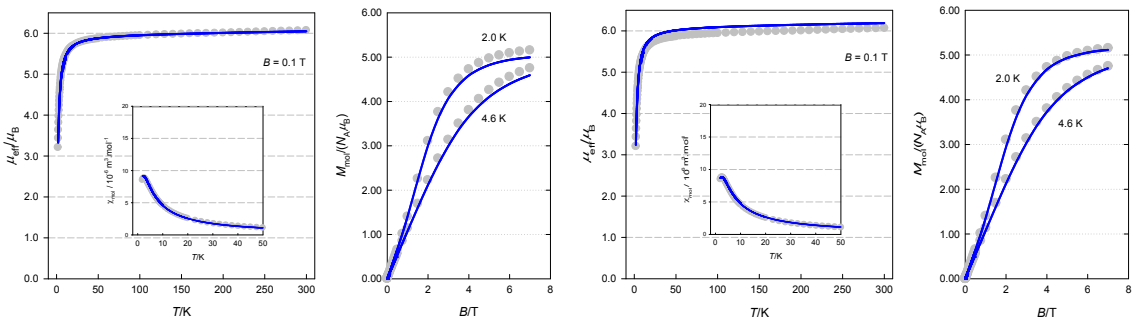

Figure S4.2 Magnetic functions for **2** (left two frames: alternative with negative D, right frames: positive D): effective magnetic moment *vs* temperature (left), magnetization *vs* magnetic field (right), magnetic susceptibility *vs* temperature (inset); grey circles: experimental data, solid line: fitted.

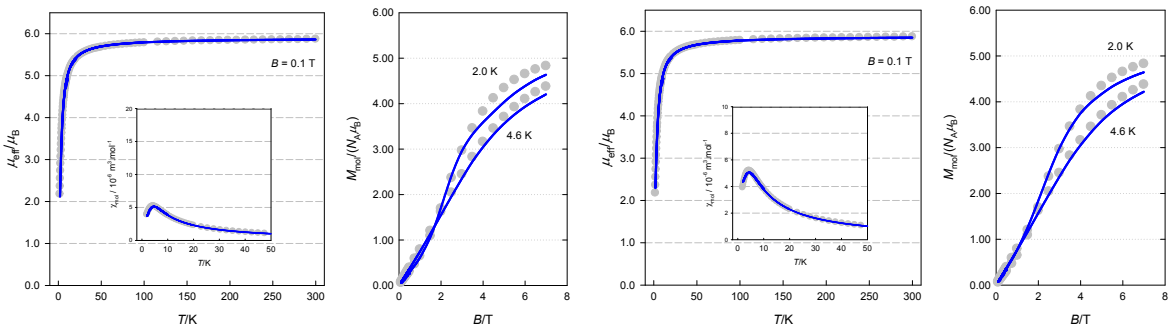

Figure S4.3 Magnetic functions for **3** (left two frames: alternative with negative D, right frames: positive D):effective magnetic moment *vs* temperature (left), magnetization *vs* magnetic field (right), magnetic susceptibility *vs* temperature (inset); grey circles: experimental data, solid line: fitted.

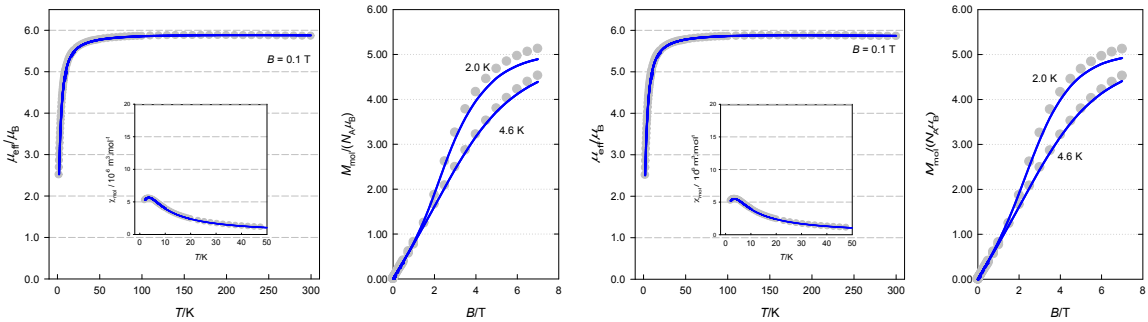

Figure S4.4 Magnetic functions for **4** (left two frames: alternative with negative D, right frames: positive D): effective magnetic moment *vs* temperature (left), magnetization *vs* magnetic field (right), magnetic susceptibility *vs* temperature (inset); grey circles: experimental data, solid line: fitted.

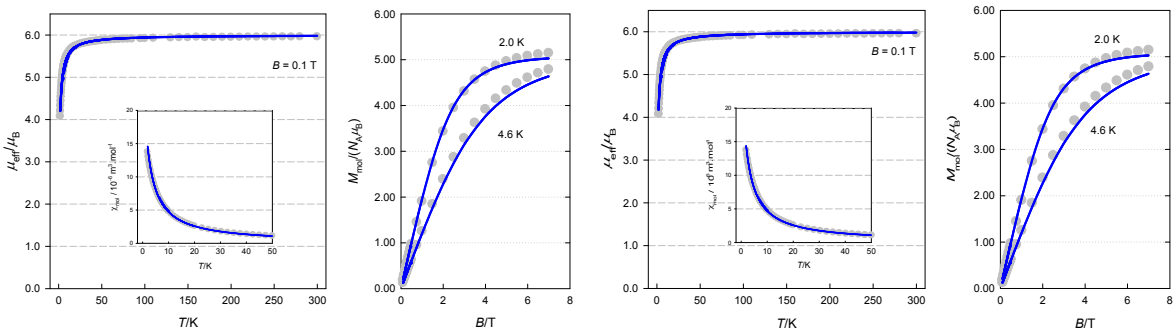

Figure S4.5 Magnetic functions for **5** (left two frames: alternative with negative D, right frames: positive D): effective magnetic moment *vs* temperature (left), magnetization *vs* magnetic field (right), magnetic susceptibility *vs* temperature (inset); grey circles: experimental data, solid line: fitted.

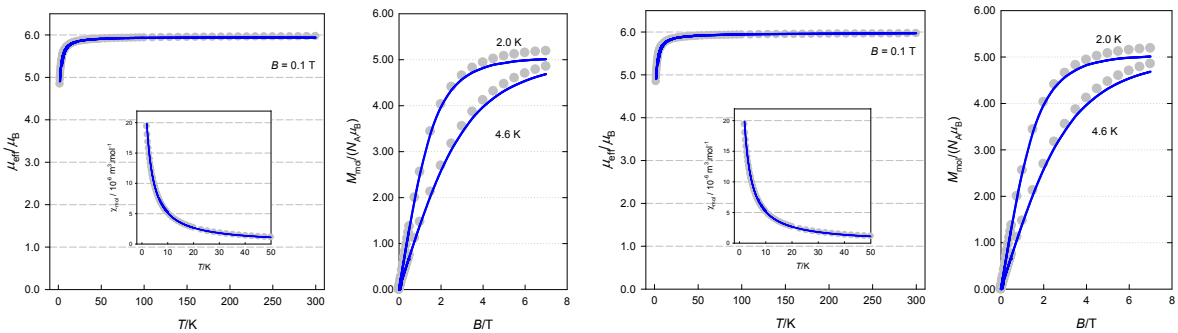

Figure S4.6 Magnetic functions for **6** (left two frames: alternative with negative D, right frames: positive D): effective magnetic moment *vs* temperature (left), magnetization *vs* magnetic field (right), magnetic susceptibility *vs* temperature (inset); grey circles: experimental data, solid line: fitted.

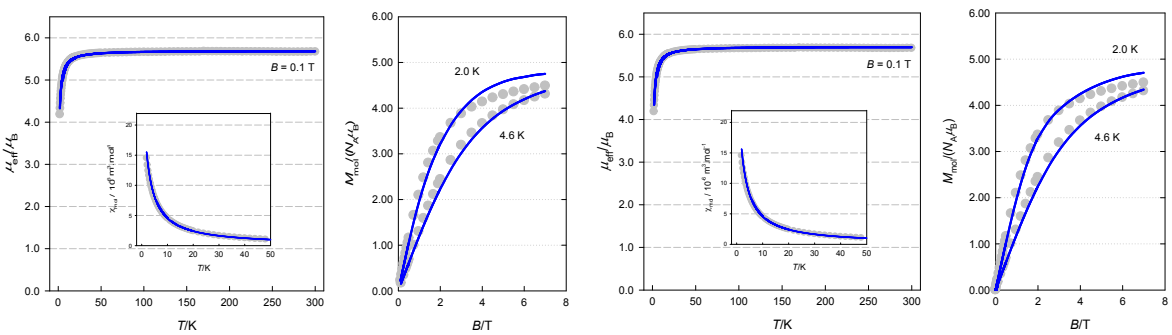

Figure S4.7 Magnetic functions for **7t** (left two frames: alternative with negative D, right frames: positive D): effective magnetic moment *vs* temperature (left), magnetization *vs* magnetic field (right), magnetic susceptibility *vs* temperature (inset); grey circles: experimental data, solid line: fitted.

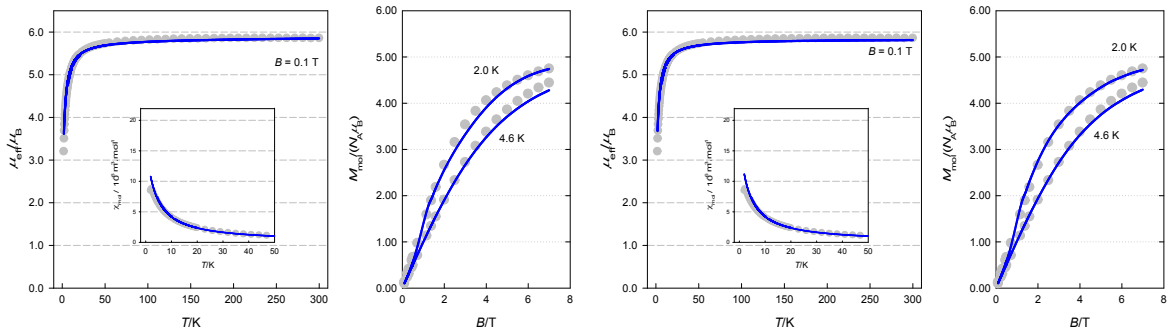

Figure S4.8 Magnetic functions for **7c** (left two frames: alternative with negative D, right frames: positive D): effective magnetic moment *vs* temperature (left), magnetization *vs* magnetic field (right), magnetic susceptibility *vs* temperature (inset); grey circles: experimental data, solid line: fitted.

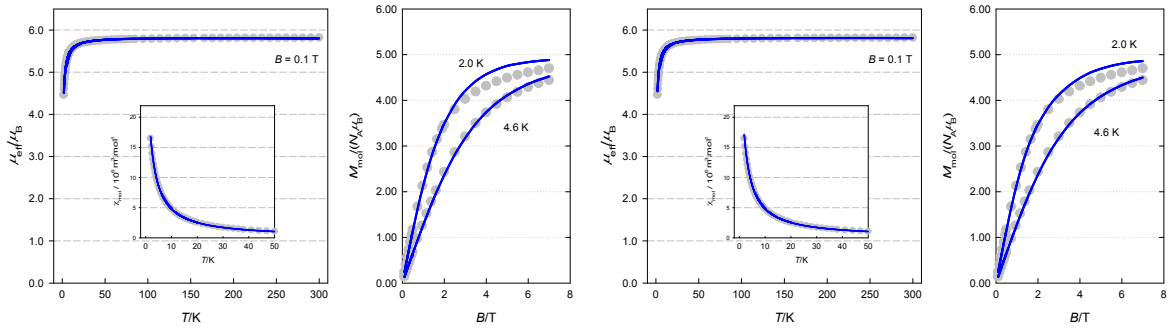

Figure S4.9 Magnetic functions for **8** (left two frames: alternative with negative D, right frames: positive D): effective magnetic moment *vs* temperature (left), magnetization *vs* magnetic field (right), magnetic susceptibility *vs* temperature (inset); grey circles: experimental data, solid line: fitted.

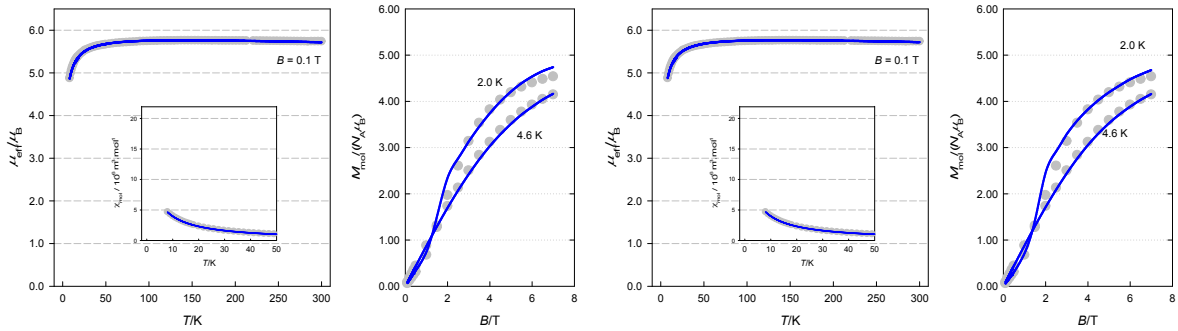

Figure S4.10 Magnetic functions for **9** (left two frames: alternative with negative D, right frames: positive D): effective magnetic moment *vs* temperature (left), magnetization *vs* magnetic field (right), magnetic susceptibility *vs* temperature (inset); grey circles: experimental data, solid line: fitted.

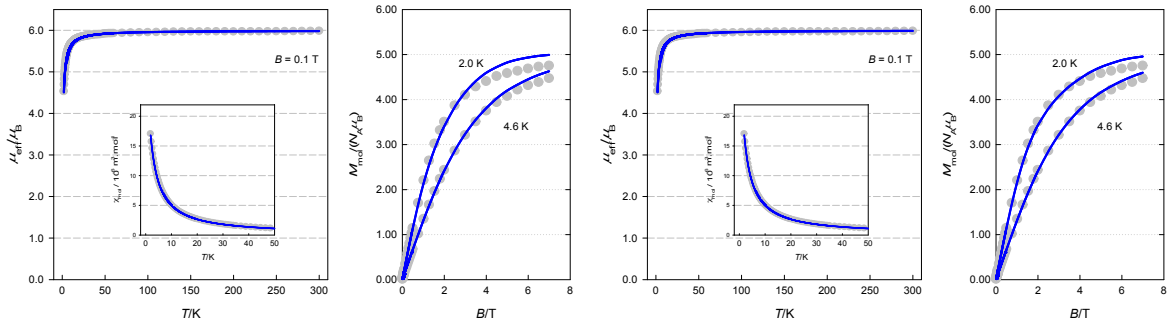

Figure S4.11 Magnetic functions for **10** (left two frames: alternative with negative D, right frames: positive D): effective magnetic moment *vs* temperature (left), magnetization *vs* magnetic field (right), magnetic susceptibility *vs* temperature (inset); grey circles: experimental data, solid line: fitted.

Table S4.1 Summary of magnetic parameters of compounds **1-10**, for the alternative with **negative** value of the *D* parameter.

Complex	J(-)/cm^{-1}	g(-)	D(-)/cm^{-1}	(zj)(-)/cm^{-1}	χ_{TIM}(-) [a]	$R(\chi)/R(M)$
1	-0.30	2.07	-0.43	-0.12	2.18	0.031/0.026
2	-0.44	2.02	-0.15	0.00	5.61	0.023/0.033
3	-0.56	1.99	-0.77	-0.18	0.41	0.019/0.049
4	-0.72	2.02	-0.25	0.00	-3.56	0.014/0.037
5	0.00	2.03	-0.07	-0.46	0.00	0.031/0.026
6	0.00	2.02	-0.10	-0.21	-1.05	0.013/0.030
7c	0.00	1.97	-0.75	-0.67	2.28	0.104/0.033
7t	0.00	1.93	-0.52	-0.30	-0.98	0.043/0.053
8	0.00	1.97	-0.40	-0.29	-1.83	0.011/0.037
9	0.00	2.00	-0.75	-0.89	-9.92	0.009/0.037
10	0.00	2.02	-0.56	-0.31	0.00	0.018/0.037

[a] In SI unit of 10^{-9} m^3 mol^{-1}.

Table S4.2 Summary of magnetic parameters of compounds **1-10**, for the alternative with **positive** value of the *D* parameter.

Complex	J(+)/cm^{-1}	g(+)	D(+)/cm^{-1}	(zj)(+)/cm^{-1}	χ_{TIM}(+) [a]	$R(\chi)/R(M)$
1	-0.37	2.07	0.54	0.00	3.62	0.034/0.044
2	-0.49	2.07	0.13	0.00	5.66	0.017/0.021
3	-0.62	1.98	0.74	-0.14	0.49	0.030/0.039
4	-0.73	2.02	0.11	0.00	-5.58	0.018/0.033
5	0.00	2.03	0.05	-0.48	0.00	0.025/0.027
6	0.00	2.02	0.11	-0.21	1.04	0.013/0.030
7c	0.00	1.97	0.79	-0.65	0.00	0.127/0.025
7t	0.00	1.93	0.77	-0.29	-0.60	0.047/0.042
8	0.00	1.97	0.56	-0.27	-1.07	0.022/0.027
9	0.00	2.00	0.87	-0.88	-9.83	0.006/0.040
10	0.00	2.03	0.74	-0.31	0.02	0.018/0.025

[a] In SI unit of 10^{-9} m^3 mol^{-1}.

Table S4.3 Magnetic exchange parameter obtained from DFT calculation (J_{calc}) and from fitting of magnetic data with negative (J(-)) and positive (J(+)) alternative of axial zero-field splitting parameter.

Complex	J_{calc}/cm^{-1}	J(-)/cm^{-1}	J(+)/cm^{-1}
1	-0.19	-0.30	-0.37
2	-0.42	-0.44	-0.49
3	-0.57	-0.60	-0.62
4	-0.54	-0.72	-0.73

Table S4.4 Spin Hamiltonian parameters for the selected high spin mononuclear [Fe(L)X] complexes (where X= Cl^- or pseudhalido terminal ligands) with different type of pentadentate SB ligands

Complex	$J(+)/cm^{-1}$	$g(+)$	$D(+)/cm^{-1}$	$J(-)/cm^{-1}$	$g(-)$	$D(-)/cm^{-1}$	Aliphatic part of L
1[a]	-0.37	2.07	+0.54	-0.30	2.07	-0.43	DET
2[a]	-0.49	2.07	+0.13	-0.44	2.02	-0.15	DET
3[a]	-0.62	1.98	+0.74	-0.56	1.99	-0.77	DET
4[a]	-0.73	2.02	+0.11	-0.72	2.02	-0.25	DET
5[a]	0.00	2.03	+0.05	-	2.03	-0.07	PET
6[a]	-	2.02	+0.11	-	2.02	-0.10	PET
7c[a]	-	1.97	+0.79	-	1.97	-0.75	DPT
7t[a]	-	1.93	+0.77	-	1.93	-0.52	DPT
8[a]	-	1.97	+0.56	-	1.97	-0.40	DPT
9[a]	-	2.00	+0.87	-	2.00	-0.75	DPTM
10[a]	-	2.03	+0.74	-	2.02	-0.56	DPTM
C1[22]	-0.48	1.96	+0.30	-0.51	1.97	-0.09	DET
C2[22]	-0.48	1.95	+0.70	-0.45	1.94	-0.53	DET
C3[22]	-	1.96	+1.01	-	1.96	-0.81	PET
C4[22]	-	1.89	+0.94	-	1.87	-0.63	DPTM
C5[22]	-0.76	1.99	+0.63	-0.62	1.95	-0.67	DET
C6[22]	-	1.98	+0.50	-	1.98	-0.37	PET
C7[22]	-	1.98	+1.03	-	1.98	-0.72	DPTM
C8[22]	-	1.88	+0.72	-	1.88	-0.59	DPT
C9[22]	-	1.94	+0.91	-	1.94	-0.71	DPTM
C10[22]	-	1.98	+1.10	-	1.97	-0.69	DPTM
C11[22]	-	2.01	+1.22	-	2.00	-0.88	DPTM
C12[22]	-	1.99	+0.64	-0.22	1.97	-0.01	PET
3·C_3H_6O[23]	-	2.02	+0.75	-	2.02	0.66	PET
C1[24]	-0.522	1.96	+0.65	-0.491	1.97	-0.57	DET
C2[24]	-0.678	1.96	+0.95	-0.707	1.94	-0.75	DET
C3[24]	-0.371	2.00	+0.81	-0.312	1.97	-0.67	DET
C4[24]	-0.311	1.98	+0.58	-0.312	1.98	-0.53	DET
C5[24]	-0.423	2.00	+0.33	-0.374	1.98	-0.37	DET
C6[24]	-0.390	2.00	+0.48	-0.370	1.98	-0.37	DET
C7[24]	-0.276	1.96	+0.73	-0.224	1.93	-0.56	DET
C8[24]	-	1.90	+0.44	-	1.90	-0.42	DPT
C9[24]	-	1.95	+0.70	-	1.95	-0.60	DPTM
3[25]	1.98		+1.07	-	-	-	PET
4[25]	2.03		+0.11	-	-	-	PET
5[25]	2.01		+0.60	-	-	-	PET
6[25]	-	-	-	-0.56	2.01	-0.50	DET
2a(dimer)[26]	− 0.30	1.98	+0.78	-	-	-	PET
2a (1D chain)[26]	− 0.18	1.98	+0.68	-	-	-	PET
2b[26]	− 0.40	2.00	+1.18	-	-	-	DPT
2c[26]	− 0.20	2.04	+0.61	-	-	-	PET
2d[26]	− 0.38	2.01	+1.35	-	-	-	DET

[a]This article

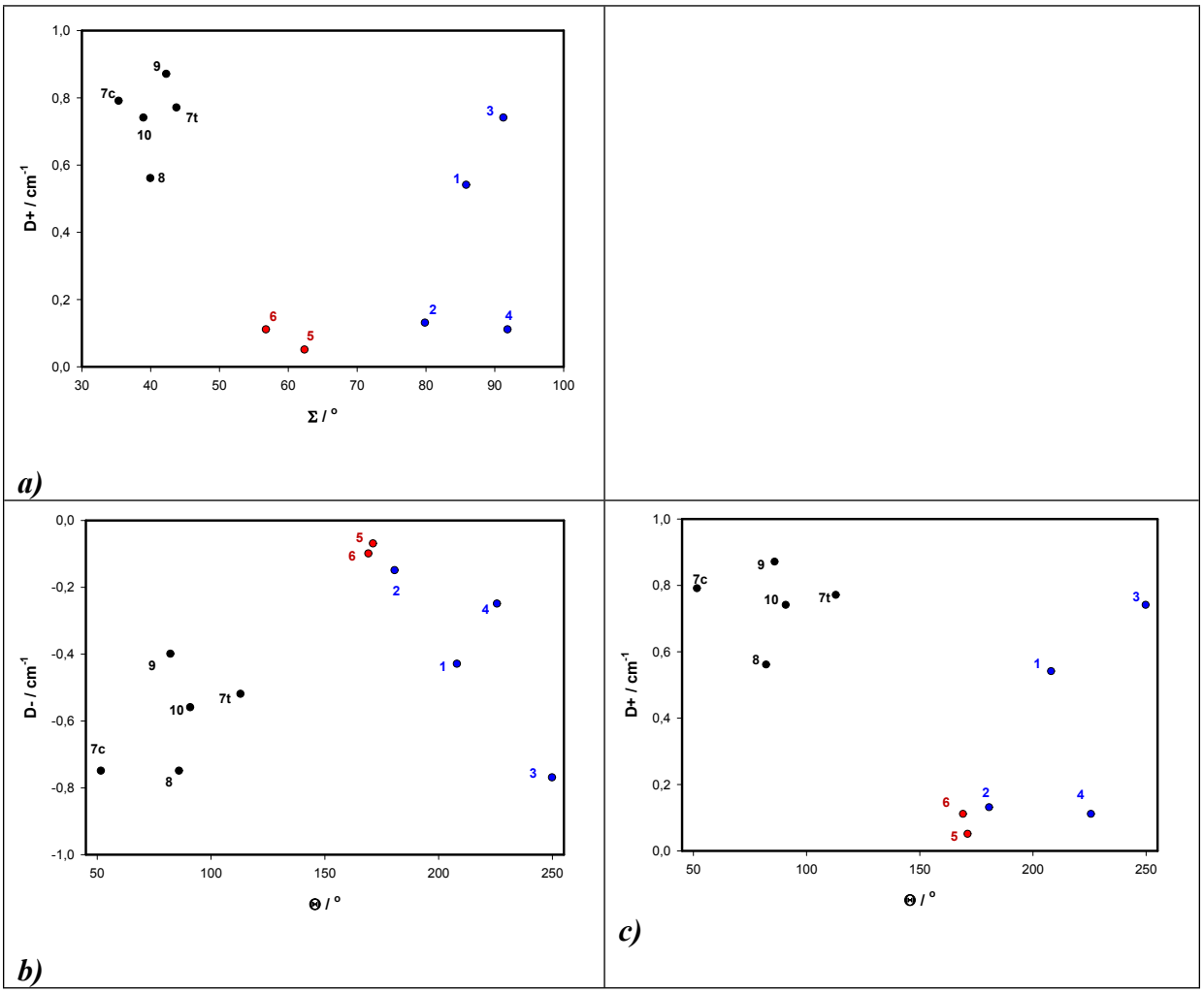

Figure S4.12 Magnetostructural correlation of reported compounds **1-10**: Evolution of D+ upon the variation of Σ distortion parameter (***a***). Evolution of D- (***b***) and D+ (***c***) parameters upon the variation of Θ distortion parameter. Datapoints of compounds containing the shortest DET aliphatic part are marked with blue, PET with red and DPT or DPTM with black colour.

S5. EPR spectra of reported compounds

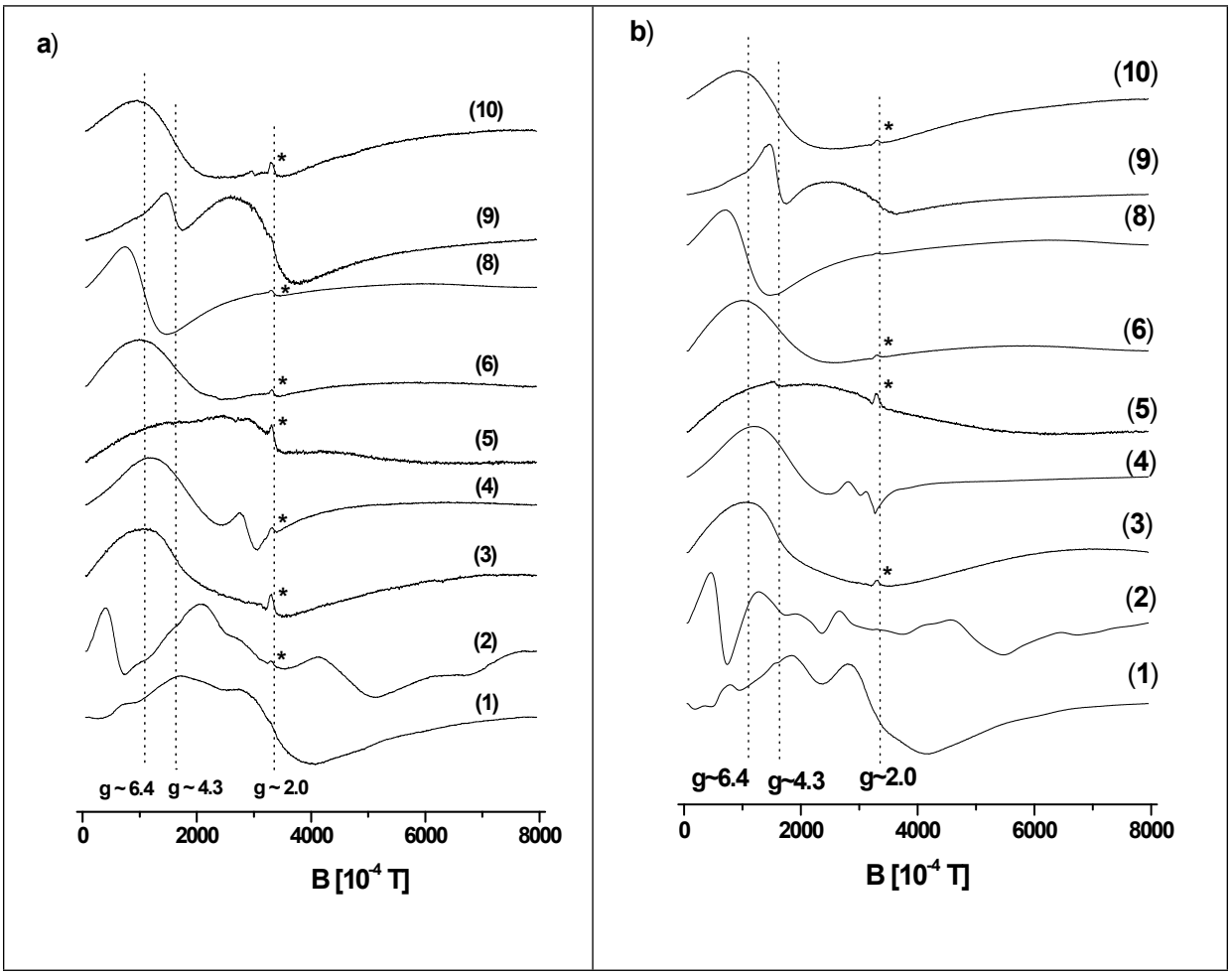

Figure S5.1 The first derivative X-band EPR spectra of complexes **1** - **6** and **8** - **10** measured at **a**) 293 K and **b**) 98 K. For illustration, effective g-factors expected for rhombic extreme (E/D = 1/3) and axial extreme (E/D ≈ 0) are indicated.

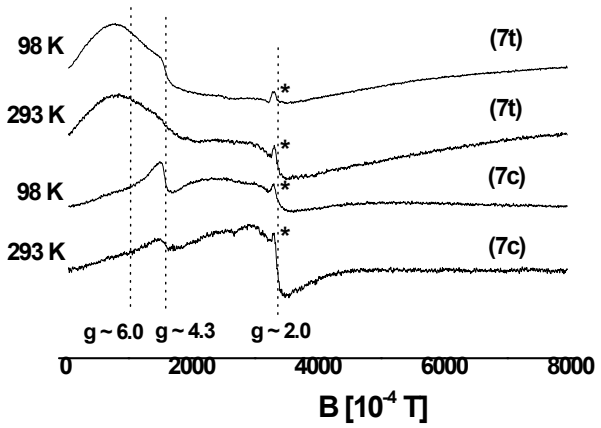

Figure S5.2 The first derivative X-band EPR spectra of complexes **7c** and **7t** measured at 293 K and 98 K. For illustration, effective g-factors expected for rhombic extreme (E/D = 1/3) and axial extreme (E/D ≈ 0) are indicated.

S6. Electrochemistry

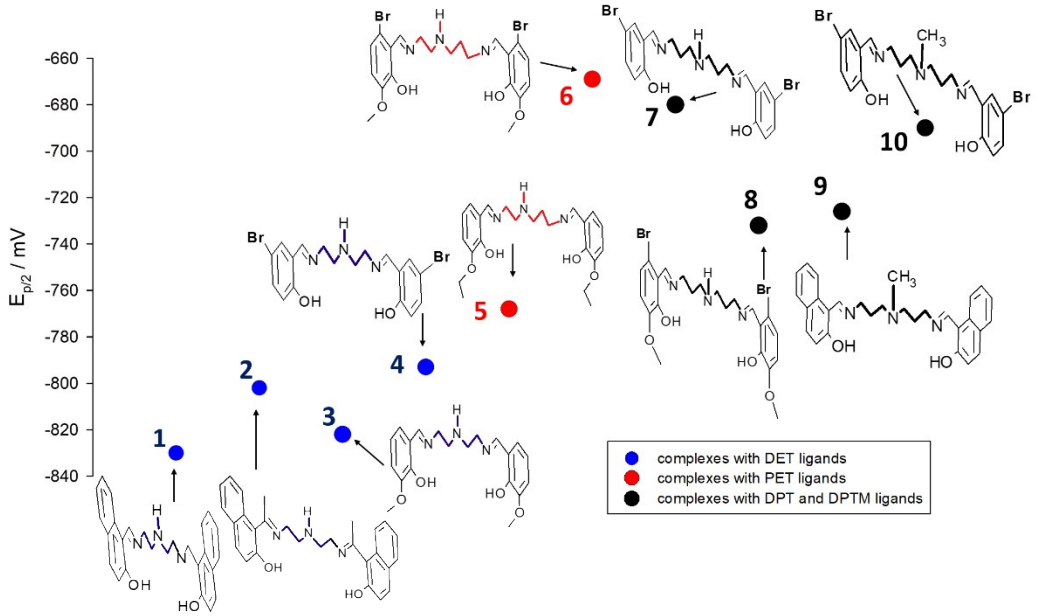

Figure S6.1 Evolution of $E_{p/2}$-$E_{p/2}$(Fc) potential within the series of complexes **1-10** with the visualized corresponding Schiff base ligands.

$$\begin{tikzcd}
\mathrm{Ox(g)} + \mathrm{e}^- \arrow[rr, "\Delta G^{o}_{g}"] \arrow[dd, "\Delta G^{o}_{solv}(\mathrm{Ox})"'] & & \mathrm{Red(g)} \arrow[dd, "\Delta G^{o}_{solv}(\mathrm{Red})"] \\
& & \\
\mathrm{Ox(solv)} + \mathrm{e}^- \arrow[rr, "\Delta G^{o}_{solv}"] & & \mathrm{Red(solv)}
\end{tikzcd}$$

Figure S6.2 Born-Haber cycle used to calculate redox potential.

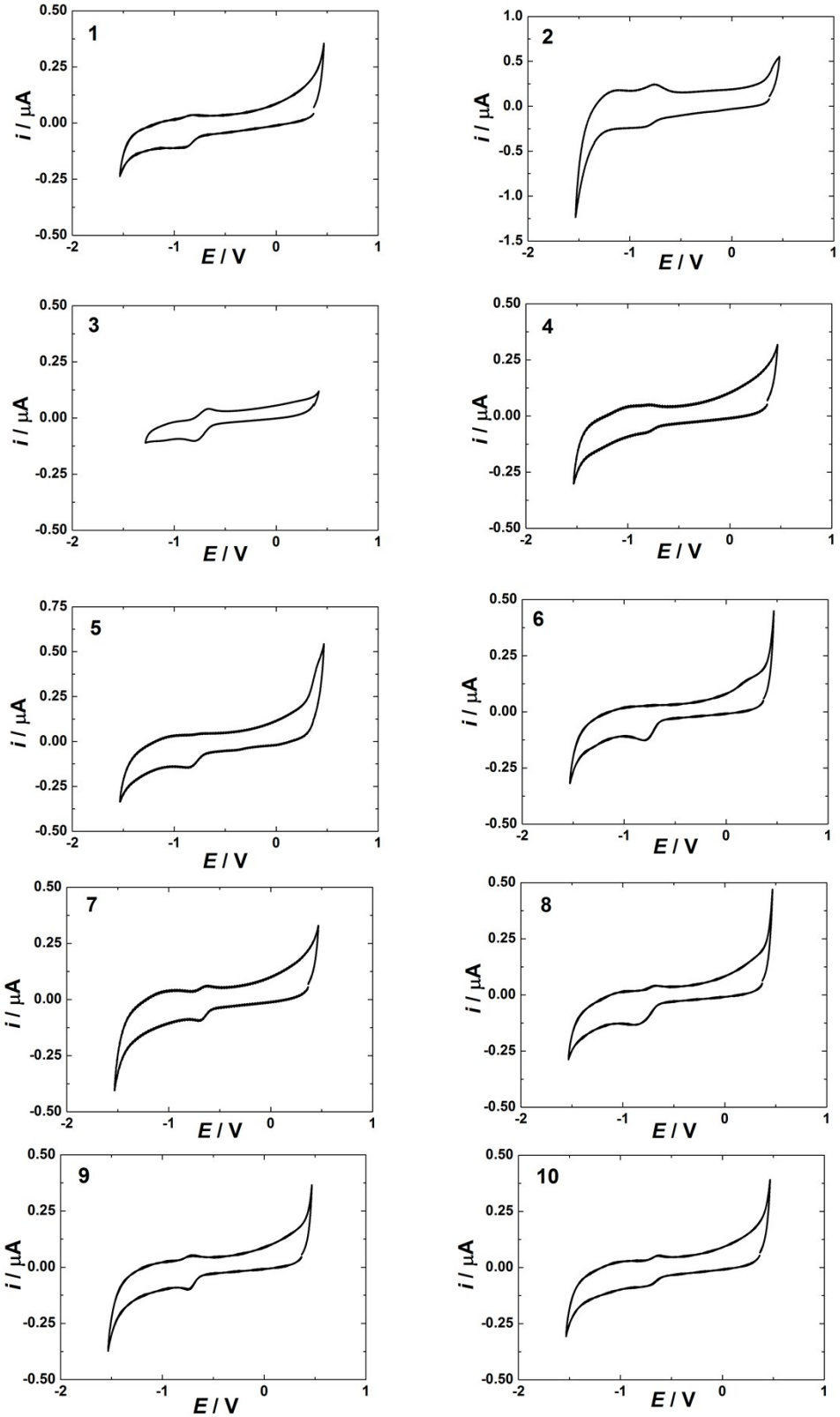

Figure S6.3 Cyclic voltammograms of respective compounds. All potentials are referred to the Fc/Fc^+ couple.

References

1 G. M. Sheldrick. *Acta Crystallogr. Sect. A* **2008**. *64*. 112.

2 G. M. Sheldrick. *Acta Crystallogr.. Sect. A* **2015**. *71*. 3.
3 M. C. Burla. R. Caliandro. M. Camalli. B. Carrozzini. G. L. Cascarano. C. Giacovazzo. M. Mallamo. A. Mazzone. G. Polidori. R. Spagna. *J. Appl. Crystallogr.* **2012**. *45*. 357.
4 O. V. Dolomanov. L. J. Bourhis. R.J. Gildea. J. A. K. Howard. H. Puschmann. *J. Appl. Crystallogr.* **2009**. *42*. 339.
5 L. J. Farrugia. *J. Appl. Crystallogr.* **2012**. *45*. 849.
6 B. Rees. L. Jenner. M. Yusupov. *Acta Crystallogr. Sect. D* **2005**. *61*. 1299.
7 A. L. Spek. *Acta Crystallogr. Sect. D* **2009**. *65*. 145.
8 a) O. Kahn, Molecular Magnetism, VCH, New York, **1993**. b) R. Boča, Theoretical Foundations of Molecular Magnetism, Elsevier, Amsterdam, **1999**.
9 H. Thiele, J. Etstling, P. Such, P. Hoefer, 1992, WINEPR, Germany, Bruker Analytic Gmb.
10 R. T. Weber, 1995, WINEPR SimFonia, Billerica, USA, EPR Division, Bruker Instr. Inc.
11 A.Ozarowski, "Spin", National High Magnetic Field Laboratory Florida, USA, free available on: http://myweb.fsu.edu/aozarows/EPR/, 11-Aug-2014
12 W. R. Hagen, 2009 Biomolecular EPR spectroscopy, CRC Press, Taylor & Francis Group, Boca Raton.
13 F. Neese *WIREs Comput. Mol. Sci.* **2018**, 8:e1327. doi: 10.1002/wcms.1327.
14 X. Xu, W. A. Goddard III *Proc. Natl. Acad. Sci. USA* **2004**, *101(9)*, 2673.
15 T. Nakajima *Chem. Rev.* **2012**, *112(1)*, 385.
16 a) F. Wiegend, L. Ahlrichs *Phys. Chem. Chem. Phys.* **2005**, *7*, 3297; b) A. Schaefer, H. Horn, R. Ahlrichs *J. Chem. Phys.* **1992**, *97*, 2571; c) A. Schaefer, C. Huber, R. Ahlrichs, *J. Chem. Phys.* **1994**, *100*, 5829.
17 R. Izsak, F. Neese *J. Chem. Phys.* **2011**, *135*, 144105
18 G. L. Stoychev, A. A. Auer, F. Neese *J. Chem. Theory Comput.* **2017**, *13*, 554.
19 S. Grimme, J. G. Brandenburg, C. Bannwarth, A. Hansen *J. Chem. Phys.* **2015** *143*, 054107.
20 (a) E. Van Lenthe,; E.J. Baerends,; J.G. Snijders, Relativistic regular two-component Hamiltonians. *J. Chem. Phys*. **1993**, *99*, 4597–4610. (b) C. Van Wüllen, Molecular density functional calculations in the regular relativistic approximation: Method,application to coinage metal diatomics, hydrides, fluorides and chlorides, and comparison with first-order relativistic calculations. *J. Chem. Phys.* **1998**, *109*, 392–399.
21 D.A.Pantazis,; X.-Y. Chen,; C.R. Landis,; F. Neese, All-Electron Scalar Relativistic Basis Sets for third-row Transition Metal Atoms. *J. Chem. Theory Comput.* **2008**, *4*, 908–919.
22 L. Pogány, J. Moncol, J. Pavlik, M. Mazúr, I. Šalitroš, *ChemPlusChem* 2019, **84**, 358–367.
23 L. Pogány, B. Brachňaková, J. Moncoľ, J. Pavlik, I. Nemec, Z. Trávníček, M. Mazúr, L. Bučinský, L. Suchánek, I. Šalitroš, *Chem. Eur. J.* 2018, **24**, 5191 – 5203.
24 L. Pogány, J. Moncol, J. Pavlik, I. Šalitroš, *New J. Chem.* 2017, **41**, 5904-5915
25 P. Masárová, P. Zoufalý, J. Moncol, I. Nemec, J. Pavlik, M. Gembický, Z. Trávníček, R. Boča, I. Šalitroš, *New J. Chem.*, 2015, **39**, 508-519.
26 I. Šalitroš, R. Boča, R. Herchel, J. Moncol, I. Nemec, M. Ruben, F. Renz, *Inorg. Chem.* 2012, **51**, 12755 – 12767.